

AperTO - Archivio Istituzionale Open Access dell'Università di Torino

Preparation of polymeric hybrid nanocomposites based upon PE and silica

This is the author's manuscript

Original Citation:

Availability:

This version is available <http://hdl.handle.net/2318/63542> since 2016-11-16T12:23:37Z

Published version:

DOI:10.1016/j.polymer.2009.04.012

Terms of use:

Open Access

Anyone can freely access the full text of works made available as "Open Access". Works made available under a Creative Commons license can be used according to the terms and conditions of said license. Use of all other works requires consent of the right holder (author or publisher) if not exempted from copyright protection by the applicable law.

(Article begins on next page)



UNIVERSITÀ DEGLI STUDI DI TORINO

This Accepted Author Manuscript (AAM) is copyrighted and published by Elsevier. It is posted here by agreement between Elsevier and the University of Turin. Changes resulting from the publishing process - such as editing, corrections, structural formatting, and other quality control mechanisms - may not be reflected in this version of the text. The definitive version of the text was subsequently published in *Polymer* 50 (2009) 2595–2600

You may download, copy and otherwise use the AAM for non-commercial purposes provided that your license is limited by the following restrictions:

- (1) You may use this AAM for non-commercial purposes only under the terms of the CC-BY-NC-ND license.
- (2) The integrity of the work and identification of the author, copyright owner, and publisher must be preserved in any copy.
- (3) You must attribute this AAM in the following format: Creative Commons BY-NC-ND license (<http://creativecommons.org/licenses/by-nc-nd/4.0/deed.en>), doi:10.1016/j.polymer.2009.04.012

Preparation of hybrid polymeric nanocomposites based upon PE and silica

Silvia Barus¹, Marco Zanetti^{1*}, Massimo Lazzari^{1,2}, Luigi Costa¹

¹*IFM Chemistry Department and Nanostructured Interface and Surface (NIS) Centre of Excellence,
Università degli Studi di Torino, via Pietro Giuria 7, 10125 Torino, Italy*

²*Department of Physical Chemistry, Faculty of Chemistry, University of Santiago de Compostela,
15782, Santiago de Compostela, Spain*

* Corresponding author:

Tel.: +39-011-670-7554; fax: +39-011-670-7855.

E-mail address: marco.zanetti@unito.it (M. Zanetti).

Abstract

In this study is described the realization of nanocomposites based on a dispersion of nanoscopic silica particles in a polyethylene matrix. There is explained the realization of an hybrid material promoting the formation of covalent bonding between the inorganic phase and the polymeric organic matrix. In order to do this and to enhance the miscibility between the two phases, coupling agents have been used. Silane coupling agents containing vinyl groups have been utilized; they are able, after an electron beam radiation treatment, to react with themselves or with the matrix forming a crosslinking. The morphology and thermo-oxidative properties were investigated.

Keywords: polyethylene (PE), nanoscopic silica, hybrid nanocomposite, thermoxidation

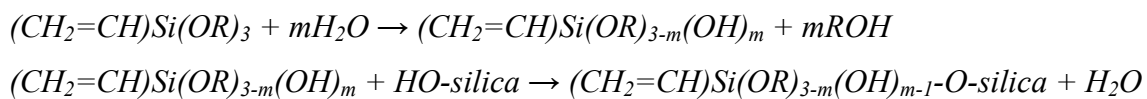
1. INTRODUCTION

The use of organic or inorganic fillers has become ubiquitous in polymeric systems [1]. Polymer composites are manufactured commercially for many applications such as sport goods, aerospace components, automobiles, etc. In the last years, there has been a strong emphasis on the development of polymeric nanocomposites, especially in the case of clays fillers where at least one of the dimensions of the filler material is of the order of nanometers [2 - 4]. It has been observed that the transition from microparticles to nanoparticles may yields dramatic changes in physical properties. These improvements can include high modulus [5], increased strength and heat resistance [6], decreased gas permeability [7, 8] and flammability [9 - 11]. In general, the unique combination of the nanomaterial characteristics, such as size, mechanical properties, and low concentrations necessary to effect change in a polymer matrix, coupled with the advanced characterization and simulation techniques now available, have generated much interest in the field. In addition, many polymer nanocomposites can be fabricated and processed in ways similar to that of conventional polymer composites, making them particularly attractive from a manufacturing point of view [12-15].

Nanoscale materials have a large surface area for a given volume. Since many important chemical and physical interactions are governed by surfaces and surface properties, a nanostructured material can have substantially different properties from a larger-dimensional material of the same composition. However, a homogeneous dispersion of nanoparticles in a polymeric matrix is a very difficult task due to the strong tendency of nanoparticles to agglomerate. Consequently, the so-called nanoparticle filled polymers sometimes contain a number of clusters of particles and exhibit properties even worse than conventional particle/polymer systems. To break down these nanoparticle agglomerates and to produce nanostructured composites, many researchers focus on the approaches of in-situ polymerization of monomers in the presence of nanoparticles, such as the sol-gel process [13] and the intercalation polymerization technique [5,16]. By examining the current technical level and the feasibility of the available processing methods, it can be concluded that the melt compounding techniques for the preparation of conventionally filled polymers is still the most convenient way when nanoparticles are proposed to replace the micron-scale fillers for the purposes of performance enhancement without variation of processability and density of the resultant composites [17]. The problem is that the agglomerates of nanoparticle are difficult to be disconnected by the limited shear forces in polymer melts, characterized by a high viscosity during melt mixing, as well as the poor interaction between the hydrophilic fillers and the hydrophobic matrix. Besides the dispersion status promotion, a lot of emphasis should be focussed on the

modification of the agglomerates themselves by means of a special surface treatment of the nanoparticles.

In this paper is described the realization of nanocomposites based on a dispersion of nanoscopic silica particles in a polyethylene matrix. The second intend of this work is the realization of an hybrid material promoting the formation of covalent bonding between the inorganic phase and the polymeric organic matrix. In order to do this and to enhance the miscibility between the two phases, coupling agents have been used. Silane coupling agents containing vinyl groups have been utilized; they are able, after a proper treatment, to react with themselves or with the matrix forming a crosslinking. We investigated two types of commercial silica, fumed silica and silicon dioxide nanopowder, in a matrix of high density polyethylene. The preparation proceeded in three steps: in first place, the functionalization of silica surface with coupling agents by sol-gel process:



Secondly, the melt-blending of modified filler with polymer and, finally, the formation of chemical bonding between matrix and filler through a free radical reaction, promoted by high energy radiation. High energy radiations create radicals onto polymer chains, which are able to react easily and rapidly with reactive groups present on silica surface (C-C double bonds), which have been introduced by silylation (fig. 1).

The so formed composites were then characterized and the chemical interaction between the matrix and nanoparticles during the irradiation procedure and possible morphological changes induced by the addition of the nanoparticles are discussed in detail.

Thermal oxidation of the obtained nanocomposites has been studied by thermogravimetry.

2. EXPERIMENTAL

2.1 Materials

High density polyethylene (PE), Eraclene ML-70, melt flow index 2.8 g/10 min, produced by Polimeri Europa, was used as matrix for this work. The silica used to prepare nanocomposites were Silicon Dioxide Nanoparticles (NS) (Sigma-Aldrich), which are spheres of 15-20 nm diameter and density of 2.2 g/cm³, with a specific area of 140-180 m²/g, and Fumed Silica (FS), (Sigma-Aldrich), consisting of pyrogenic colloidal SiO₂ with an average primary particles size of 7 nm and density of

2.2 g/cm³. In FS primary particles are sintered together forming a three-dimensional branched chain aggregate with a length of approximately 0.2–0.3 microns. Typically those aggregated leads to further entanglement of the chains, termed agglomeration with a specific area of 390±40 m²/g. Silane coupling agents (SCA), vinyltrimethoxysilane (VTMS), vinyltriethoxysilane (VTES) were produced by Sigma-Aldrich and used as received.

2.2 Silylation of silica surface

The grafting onto silica surface of silane coupling agents was carried out by sol-gel process [18]. Before being mixing with SCA, nanoparticles were preheated at 100°C under vacuum overnight to eliminate possible absorbed water on the surface. To 10 g nano-sized filler, intensively stirred in boiling acetone, first 5 g coupling agent and then 0,15 g maleic anhydride (MA) and 0,0225 ml of water, were added. MA has been used as acid catalyst for silylation reaction. The mixture was refluxed for 24 h under air and then oven-dried under vacuum at 130°C overnight to volatilize from the surface all unattached silane. The absence of unreacted silane and silylation coverage were determined by thermogravimetric analysis (TGA) (Hi-Res TGA 2950 balance, TA Inc., with alumina pan in a 100 cm³/min nitrogen or air flow and with a 10°C/min heating ramp from room temperature up to 800°C). Silylation coverage (n_s) was calculated [19] as

$$n_s = 10^6 \times (\Delta m_s / (m_s) (S_s) (MW_{silane}))$$

where n_s is the silylation coverage ($\mu\text{mol}/\text{m}^2$), Δm_s is silylation weight gain for the support (g) and measured in TGA, m_s is the mass of the support material (g), S_s is the specific surface area of the support (m^2/g), and MW_{silane} is the molecular weight of the bonded silane molecule (g/mol). It is important to note that, as a silane unit hydrolyzes and/or condenses, the effective molecular weight associated with silane units will decrease. The average molecular weight, for example, for each VTMS unit can theoretically be as high as 117 g/mol for the case of monolayer coverage and as low as 55 g/mol for the case of complete hydrolysis and condensation in a vinyltrialkoxysilane network. ²⁹Si MAS NMR spectra, ¹³C MAS NMR spectra and ATR (Dura Sampl IR II, Smiths assembled in a Perkin-Elmer Spectrum 100 Fourier transform infrared spectroscope (FTIR), equipped with a DTGS detector) spectra were utilized to characterize change in nanoparticle surfaces and to verify grafting type. All solid state NMR measurements were recorded on a Jeol GX 270 equipped with a Doty probe operating at 270.0 MHz for ¹H, 67.8 MHz for ¹³C and 53.5 MHz for ²⁹Si. A standard cross-polarization pulse sequence has been used with a contact time of 3-3.5 ms, a 90° pulse of 3.4 μs , recycle delays of 10-15 s and a number transients of 1000 and 4000 for ¹³C and ²⁹Si respectively. Cylindrical 5 mm o.d. zirconia rotors with sample volume of 120 μl were employed and spun at 5.0

kHz. ^{13}C chemical shifts were referenced via the methyl resonance (17.4 ppm) of solid hexamethylbenzene while ^{29}Si chemical shifts were referenced via solid kaolinite (-91.2 ppm).

2.3 Preparation of hybrid nanocomposites and their characterization

Composite of PE filled with 5 wt% of modified silica were prepared by melt compounding using a Brabender internal mixer AEV330. The manufacturing temperature was kept at 160°C and the screw speed amounted to 60 rpm for 10 min. The specimens were then pressed at 180±5°C and 100 bar for 5 min in a press to obtain 100x100x50 mm plates. Compounds of PE and PE-unmodified silica were prepared in the same conditions to be used as references.

Specimens were cured with doses varied between 50 and 150 kGy, under nitrogen atmosphere, by using electron beams. E-beam irradiation was performed with a 10 MeV accelerator (Bioster, Seriate, Italy), operating at 25 kW power, with a dose rate of 6×10^4 kGy/h, at room temperature.

The distribution of silica particles in composites was studied recording images on a Philips CM-12 TEM operated at an accelerating voltage of 120 kV. Samples were embedded in epoxy resin and cured at 60°C overnight. Thin sections (100 nm) were cut using a Leica Ultracut UCT ultramicrotome and a diamond knife at room temperature. No staining was performed on the microtomed sections placed onto carbon-coated copper grids. The cryo-fractured surfaces of composites were studied by a Zeiss Supra 40 field emission scanning electron microscope (FESEM) after a gilding treatment carried out by a Baltec SCD 050, working in argon atmosphere in vacuum with a 60 mA current for 60 sec, to obtain a gilt deposition of about 20-30 nm of Cr.

FTIR spectra of composites were recorded on a microscope FTIR Perkin-Elmer AutoIMAGE 2000 equipped with a MCT detector. Thin films, of about 150 μm , were obtained by microtoming specimens (Polycut microtome, Reichert-Jung). In the typical experiment, 32 scans were accumulated in transmission mode with a 4 cm^{-1} resolution. The peak at 2020 cm^{-1} , a combination band, was used as an internal standard, since it can be regarded as unaffected by minor changes in the polymer structure. At the peak at 2020 cm^{-1} , all the spectra were normalised at an absorption of 0.05, correlating to a film thickness of ca. 100 μm .

Thermo-oxidation was measured on approx. 10 mg sample in a Hi-Res TGA 2950 balance, TA Inc., with alumina pan in a $100\text{ cm}^3/\text{min}$ air flow and with a $10^\circ\text{C}/\text{min}$ heating ramp from room temperature up to 800°C .

3. RESULT AND DISCUSSION

3.1 Characterization of modified nanoparticles

The functionalization of silica nanoparticles has been studied firstly by spectroscopic techniques.

Figures 2 and 3 show the infrared spectra of FS and NS as received and modified. The presence of the modifier on the surface is confirmed by its characteristic absorption: the stretching at 1410 cm^{-1} and the in plane deformation at 1600 cm^{-1} of C=C bond of silane. These absorption are due to the reacted silane since unreacted silanes were volatilized by oven treatment under vacuum.

The solid-state NMR technique was used also to characterize the creation of chemical bonds between silica and the coupling agent and so to confirm grafting onto silica particles, and afterwards, to establish the surface structural composition of the grafted silica to compare the reactivities of the various silica silanols towards each coupling agent. With ^{13}C spectra we can control the presence of vinyl bond, while with ^{29}Si spectra the type of linking that occurs between surface and modifier.

The ^{13}C CP/MAS NMR spectra are reported in Figure 4. The resonance assignments of the corresponding chemical structures are shown on the spectra. In all cases, well-resolved spectra were obtained. Figure 5 shows the ^{29}Si CP/MAS NMR spectrum of NS-VTMS and NS-VTMS spectra.

The untreated silica generally shows three signals at -90.2 , -100.2 , and -108.9 ppm, which are respectively assigned to Q_2 geminal silanols, Q_3 free silanols, and Q_4 siloxane groups [20]. On the ^{29}Si CP/MAS NMR spectra in figure 5 of the modified silica particles, two groups of peaks are always found. As expected, the first one, from -90.0 to -110.0 ppm, is representative of the silica surface silicon atoms unmodified during the grafting process. Comparing to the silica spectrum, an increase of the signal of the siloxane groups is expected as well as a reduction of those corresponding to geminal and free silanol groups which would react during silylation. In the same time, it is interesting to see that Q_2 peak totally disappears after grafting. The second group of peaks, in the range -50 to -80 ppm, proves that the silica surface is effectively chemically modified by the alkenyltrialkoxysilane reagent. The reaction of silica surface silanols with a trialkoxysilyl functional group can lead to three types of new structures. The T_1 , T_2 , and T_3 structures are the result of the reaction of respectively one, two, and three alkoxygroups of a same silane molecule with the silanols at the silica surface [20]. In table 1 we can notice that almost all bonds are bi or tri dentate. The absence of a peak at around -60 ppm, associated to T_1 structures, exclude the presence of monodentate linkage graft.

Approximative silylation coverage may be determined using the weight loss measured by thermogravimetric analysis of modified silica nanoparticles (fig. 6), whereas a more precise value was calculated by using the molecular weight resulting from tridentate attachment (i.e., three bond with the surface per silane unit: 55g/mol for VTMS and for VTES) as proved by NMR results. The calculus had to consider also weight loss of silica only in the considered temperature range, which

in our case is about 0,3%wt for FS and 3,9%wt for NS. For FS VTMS sample, the silylation coverage is $1.84 \mu\text{mol}/\text{m}^2$; indeed for FS-VTES is about $3.03 \mu\text{mol}/\text{m}^2$. Samples containing NS are more functionalized, $5.8 \mu\text{mol}/\text{m}^2$ and $7.0 \mu\text{mol}/\text{m}^2$ for NS VTES and NS VTMS respectively, this is reasonable because NS is not aggregated and its surface sites are more accessible to reaction than in FS.

3.2 Characterization of nanocomposites

FTIR analysis

The hybrid formation after the e-beam irradiation has been studied in FTIR. In figure 7 the FTIR spectra of PE NS composites is shown. The absorptions of C=C bond (stretch at 1410 cm^{-1} and in plane deformation at 1602 cm^{-1}) confirm the presence of the coupling agent attached on silica before the irradiation. The effect of different irradiation doses are reported in the same figure. As expected, crosslinking was induced in the polymer: radicals formed by radiations move rapidly along polyethylene chains in the amorphous phase and react easily with terminal double bonds (absorption at 909 cm^{-1} decreases), creating the so called Y shaped cross-linking; furthermore the formation of radical species induces secondary reactions, which generate trans-vinylenic groups (increasing of the absorption at 965 cm^{-1}) [21]. At the same time even the vinyl group of the silane decreases (1410 and 1602 cm^{-1}) up to disappear at higher dose level, indicating the contribution to the crosslinking reaction to form the organic-inorganic hybrid. It is reasonable to consider that depending on the proximity many of these vinyl group could react together through a free radical polymerization. PE FS composites lead to the same results (not showed here).

Microscopic analyses

The morphology of the dispersion has been studied in TEM and FESEM. TEM images of all samples show a level of dispersion typical of nanocomposites (fig.8). However the degree of dispersion depends on the kind of nanosilica and on the effect of the silane coupling agent if present. In fig. 8.a and 8.c are visible PE FS and PE NS samples; the darker domains represent silica agglomerates whose dimensions are about 500 nm. In samples containing coupling agent (fig. 8.b and 8.d), smaller aggregates (100-200 nm) are visible. In the case of NS, aggregates are smaller and few single particles are also present. In both cases the presence of the silane coupling agent improved the dispersion of the nanosilica.

In Figure 9 and 10 are shown FESEM images of the surfaces of cold fracture of PE NS specimens. In the same picture we can see, on the left, the image registered with retro-diffused electrons. The pictures confirm the TEM observation showing a good level of dispersion at a large field (fig.9). In

figure 10, a number of silica aggregates appear to be “wrapped” of an organic material, forming smooth spheres of 100 nm diameter which are welded to the bulk. This sample were irradiated with electron beam, promoting the hybrid formation, and the organic material around the silica results from the free radical reaction of the vinyl terminals of VTES with the polymer chains an with them self.

Thermal degradation

Thermogravimetric Analysis (TGA), which provides information about the thermal stability and decomposition rate of materials, is an excellent technique for rapidly comparing the behaviour of materials tested with different flame retardants and in the case of clay nanocomposites demonstrated to be very sensitive to the level of dispersion.

Figure 11 and 12 show TGA curves of PE composites in air. Filled samples are more stable compared to polymer, indeed weight loss starts at higher temperatures, with an increase in stability of about 100°C. In earlier work it has been reported that in the case of polymethylmethacrylate the presence of nanosilica did not significantly change the thermal stability [22]. A slight effect of stabilization in TGA of nanosilica was observed for polypropylene by Kashiwagi et al. [23]. In the same paper the effect of nanosilica was stronger as flame retardant as observed in cone calorimeter experiment and explained in terms of physical protection: nanosilica significantly increased the polymer melt viscosity of the molten polymer during the combustion. Consequently the additives accumulated near the regressing acting as an insulation layer.

Our result indicates that PE is somewhat more sensitive to nanosilica. In particular, FS showed to be more effective than NS. Taking in mind the morphology seen in TEM images, FS nanocomposites present bigger agglomerate/aggregate. In a mechanism involving an ablative behaviour, where the aggregation of nanoparticles is required to form an efficient shield, the nanocomposites based on FS has a sort of pre-aggregation that could render more effective the shield formation. In other words the FS aggregates have an aspect ratio rendering their shear behaviour in the molten polymer similar to that observed in layered silicate nanocomposites. On the other hand the dimension of the agglomerate is away from the range of macrocomposites in which the particles are to big to be able to form the protection shield. The stabilization trend shows in figures 11 and 12 is inversely proportional to the dispersion degree observed previously. By this point of view become clear that the presence of the silane coupling agent decrease the effect of stabilization

The effect of cross-linking and covalent bond between matrix and filler on thermal oxidation of PE and PE FS VTES is shown in figure 13.

Respect to the pure polymer, the cross-linking induces a stabilization effect. In the nanocomposite the irradiation causes a further stabilization indicating a positive effect of nanoparticles to reduce thermal oxidation. However, the stabilization reached in the cross-linked nanocomposites is lower than in the non-cross-linked one, indicating that, in the latter case, the shielding effect of FS is more effective. Again this evidence is concordant with the mechanism proposed: the higher viscosity of the crosslinked polymer at high temperature and the chemical bonding between polymer chains and nanosilica interfere with their migration reducing the effectiveness of the mechanism.

In precedent works we found that the migration of nanoparticles during the burning process of clay nanocomposites is not the sole mechanism responsible of flame retardant effect. To be consistent the particles forming the shield need to be cemented together by a minimum amount of char [10]. This is particularly important in polymers such as PE that are no char former in thermal degradation. In this latter case it has been demonstrated that the clay platelet promoted the char formation [24].

In fig 14 we reported FTIR spectra of PE nanocomposite. These spectra were performed with a cell that permit to register spectra on a sample subjected to a temperature ramp (10°C/min) from room temperature (RT) to 550°C. These measures were used to check if also silica particles can promote or facilitate polymer carbonization. In particular we examined the trend of absorbances typical of aromatic compounds which may indicate the evolution of degradation process toward the formation of carbonaceous structures.

In figure 14, when temperature rises, we can notice, at 1600 cm⁻¹, the appearance of a wide absorption band assignable to aromatic C=C bonds and, in the range 1700-1760 cm⁻¹, the absorption bands of oxidized species, that are the principal products of PE thermo-oxidation. The appearance of aromatic structures in PE FS nanocomposite occurs at 300°C, while in the polymer alone (results not reported here) it occurs dozen degrees later demonstrating a sort of catalyzing effect of silica on their formation.

Another interesting aspect is that silica, acting as a shield, preserves long chain structure at elevated temperature (450°C instead of 300-350°C in polymer matrix) where dehydrogenation and cyclization reactions became possible and undergo competition with chain scission, which is the principal decomposition process for PE. The result is the formation of charred surface layer which acts insulating and shielding the material during decomposition.

4. CONCLUSION

In the present study, TEM and FESEM analyses have demonstrated that composite materials of polyethylene and nanoscopic silica don't have macroscopic aggregates but a good dispersion, so we

can say that samples are nanostructured. The functionalization of the inorganic filler is useful to obtain a better dispersion in the organic matrix and to link silica to polymer. FTIR shows that irradiated composites reticulate. Cross-linking involves both polymer chains and modified filler so the formation of hybrid is proved. TGA curves have shown that filled samples are more stable to thermo-oxidation as regards polymer. In oxidant atmosphere, analyses have demonstrated that the advantage, brought by fillers, in term of thermal stability, is included from 50 to 100°C. The stabilization is to attribute to disperse silica on polymer matrix, which acts screening oxygen effects, inducing a partial reticulation and forming a char layer.

In addition, the modification method is simple and easier to carry out because the nanoparticles possessed a higher reactivity in comparison to conventional micron-scale inorganic particles. This means that the modified nanoparticles can be effectively utilized in thermoplastics polymer than conventional particulate fillers, when using the same direct compounding technology, to obtain an improving of different properties. This behaviour could be explain by, firstly, the significant increase in the hydrophobicity of the nanoparticles due to the presence of the coupling agent which increase the filler/matrix miscibility, even though the fillers could not be dispersed completely in the form of primary nanoparticles in the polymer matrix. Secondly, the filler/matrix interaction is substantially enhanced by the entanglement of the coupling agent and the matrix polymer promoted by radiation treatment.

Acknowledgements

The authors wish to thank Dr. Michele Chierotti and Prof. Roberto Gobetto, University of Turin, for NMR analyses and discussion, Dr. Angelica Chiodoni and Politecnico of Turin for FESEM analyses, BIOSFER S.p.A., Bergamo (MI), for composites irradiation and Dr. Valentina Brunella and Dr. Pierangiola Bracco, University of Turin, for helpful discussion.

REFERENCES

- [1] F. Hussain, M. Hojjati, M. Okamoto, R. Gorga Review article: Polymer-matrix nanocomposites, Processing, Manufacturing, and Application: An Overview. *Journal of Composite Materials* 2006; 40 (17): 1511-1575.
- [2] M. Zanetti, S. Lomakin, G. Camino Polymer layered silicate nanocomposites. *Macromol. Mater. Eng.* 2000; 279: 1-9.
- [3] A. Okada, A. Usuki Twenty Years of Polymer-Clay Nanocomposites. *Macromol. Mater. Eng.* 2006; 291: 1449-1476.
- [4] S. S. Ray, M. Okamoto Polymer/layered silicate nanocomposites: a review from preparation to processing. *Prog. Polym. Sci.* 2003; 28: 1539-1641.
- [5] E.P. Giannelis Polymer Layered Silicate Nanocomposites. *Adv. Mater.* 1996; 8(1): 29-35.
- [6] E.P. Giannelis Polymer-layered silicate nanocomposites: synthesis, properties and applications. *Appl Organomet Chem* 1998; 12: 675-680.
- [7] M. A. Osman, V. Mittal, M. Morbidelli, U. W. Suter Polyurethane Adhesive Nanocomposites as Gas Permeation Barrier. *Macromolecules* 2004; 37: 7250-7257.
- [8] A. Sorrentino, M. Tortora, V. Vittoria Diffusion Behavior in Polymer–Clay Nanocomposites. *Journal of Polymer Science Part B: Polymer Physics* 2006; 44(2): 265-274.
- [9] JW. Gilman Flammability and thermal stability studies of polymer layered-silicate clay/nanocomposites. *Appl Clay Sci* 1999;15: 31-49.
- [10] M. Zanetti , T. Kashiwagi, L. Falqui, G. Camino Cone Calorimeter Combustion and Gasification Studies of Polymer Layered Silicate Nanocomposites. *Chemistry of Materials* 2002; 14: 881-887.
- [11] M. Zanetti In: Y-W. Mai, Z-Z. Yu editors. *Polymer nanocomposites: Flammability and thermal stability of polymer/layered silicate nanocomposites*. Cambridge: Woodhead Publishing Limited, 2006. p. 256.
- [12] C-L. Chiang; C-C. M. Ma In: Y-W. Mai, Z-Z. Yu editors. *Polymer nanocomposites: Phenolic resin/SiO₂ organic-inorganic hybrid nanocomposites*. Cambridge: Woodhead Publishing Limited, 2006. p. 485.
- [13] B.M. Novak Hybrid Nanocomposite Materials-Between Inorganic Glasses and Organic Polymers. *Advanced Materials* 1993; 5 (6): 422-433.
- [14] J. Wen, G.L.Wilkes Organic/Inorganic Hybrid Network Materials by the Sol-Gel Approach. *Chem. Mater.* 1996; 8: 1667-1681.

- [15] J. Pyun, K. Matyjaszewski Synthesis of Nanocomposite Organic/Inorganic Hybrid Materials Using Controlled/"Living" Radical Polymerization. *Chem.Mater.* 2001; 13: 3436-3448.
- [16] M. Alexandre; P. Dubois; T. Sun; J.M. Garees; R. Jérôme Polyethylene-layered silicate nanocomposites prepared by the polymerization-filling technique, synthesis and mechanical properties. *Polymer* 2002; 43: 2123-2132.
- [17] MZ. Rong, MQ. Zhang, YX. Zheng, HM. Zeng, R. Walter, K. Friedrich Structure-property relationships of irradiation grafted nano-inorganic particle filled propylene composites. *Polymer* 2001; 42: 167-183.
- [18] F. Bauer, H. Ernst, U. Decker, M. Findeisen, H. Glasel, H. Langguth, E. Hartmann, R. Mehnert, C. Peuker Preparation of scratch and abrasion resistant polymeric nanocomposites by monomer grafting onto nanoparticles, 1. *Macromolecular Chemistry and Physics* 2000; 201(18): 2654-2659.
- [19] W. Yoshida, R. P. Castro, J.-D. Jou, Y. Cohen Multilayer Alkoxysilane Silylation of Oxide Surfaces. *Langmuir* 2001;17:5882-5888.
- [20] D. Derouet, S. Forgeard, J. Brosse, j. Emery, j. Buzare Application of Solid-State NMR (¹³C and ²⁹Si CP/MAS NMR) Spectroscopy to the Characterization of Alkenyltrialkoxysilane and Trialkoxysilyl-Terminated Polyisoprene Grafting onto Silica Microparticles. *Journal of Polymer Science: Part A: Polymer Chemistry* 1998; 36: 437-453.
- [21] P. Bracco, V. Brunella, M.P. Luda, M. Zanetti, L. Costa Radiation-induced crosslinking of UHMWPE in the presence of co-agents: chemical and mechanical characterisation. *Polymer* 2005; 46: 10648-10657.
- [22] T. Kashiwagi, A.B. Morgan, J.M. Antonucci, M.R. VanLandingham, R. H. Harris, W.H. Awad, J.R. Shields Thermal and Flammability Properties of a Silica–Poly(methylmethacrylate) Nanocomposite. *Journal of Applied Polymer Science* 2002; 89: 2072-2078.
- [23] T. Kashiwagi, J.W. Gilman, K.M. Butler, R.H. Harris, J.R. Shields, A. Asano Flame Retardant Mechanism of Silica Gel/silica. *Fire and Materials* 2000; 24: 277-289.
- [24] M. Zanetti, P. Bracco, L. Costa Thermal degradation behaviour of PE/clay nanocomposites. *Polymer Degradation and Stability* 2004; 85: 657-665.
- [25] L. Costa, M. Avataneo, P. Bracco, and V. Brunella Char formation in polyvinyl polymers: I. Polyvinyl acetate. *Polymer Degradation and Stability* 2002; 77: 503-510.

Captions

Figure 1 Schematic representation of the reaction mechanism of hybrid formation.

Figure 2 FTIR spectra of FS and modified FS nanoparticles. In the zoomed area has been pointed out the appearance, after silylation, of the characteristic absorbances of coupling agents vinyl bond.

Figure 3 FTIR spectra of NS and modified NS nanoparticles. In the zoomed area has been pointed out the appearance, after silylation, of the characteristic absorbances of coupling agents vinyl bond.

Figure 4 ^{13}C CP MAS NMR spectra of NS silylated nanoparticles: (on the top) NS VTMS and (on the bottom) NS VTES.

Figure 5 ^{29}Si CP MAS NMR spectra of modified NS nanoparticles: (on the top) NS VTMS and (on the bottom) NS VTES.

Table 1 ^{29}Si CP/MAS NMR Analysis of the various alkenyl-bonded silica particles: silicon chemical shifts (in ppm) in relation with the grafted structures.

Figure 6 TGA traces of different modified silica nanoparticles registered in oxidant atmosphere.

Figure 7 FTIR spectra of 1800-800 cm^{-1} range of absorbances for PE composites. The decrease in intensity of vinyl absorbance when radiation dose augments, implies hybrid formation.

Figure 8 TEM images of a) PE FS, b) PE FS VTES, c) PE NS and d) PE NS VTES nanocomposites

Figure 9 FESEM image of cryo-fractured PE NS nanocomposite. The light spots represent silica aggregates.

Figure 10 FESEM image of cryo-fractured PE NS VTES 150 KGy nanocomposite. Some of the bright spots of silica aggregates (in circle) seem to be wrapped by polymer.

Figure 11 Polymer weight loss from TGA scans in air for PE and four nanocomposites containing 5 wt% of FS and modified FS.

Figure 12 TGA curves in air of PE and four nanocomposites containing 5 wt% of NS and modified NS.

Figure 13 TGA curves in air of PE and PE FS VTES nanocomposite, before and after radiation treatment.

Figure 14 FTIR spectra of PE FS nanocomposite recorded with a special cell heated from room temperature to 500°C, with a heating ramp of 10 °C/min [25].

Figures

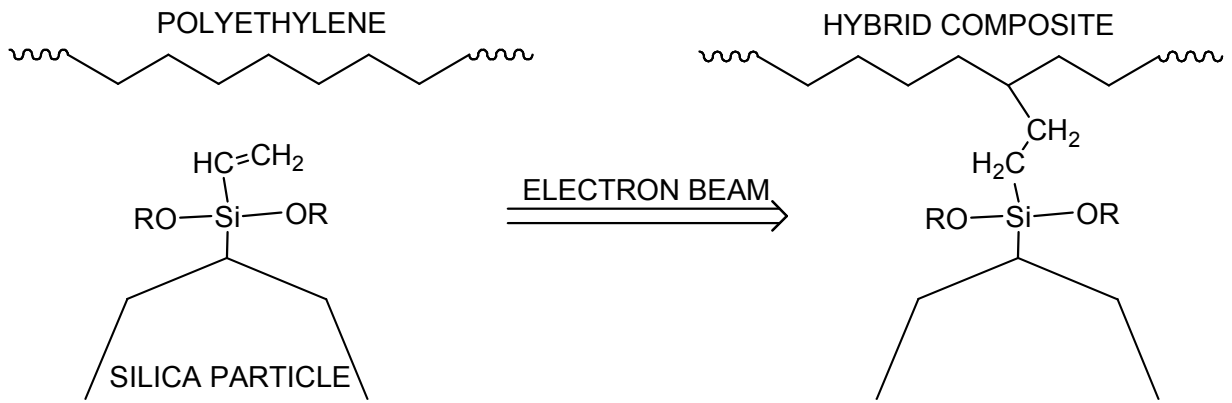


Fig.1

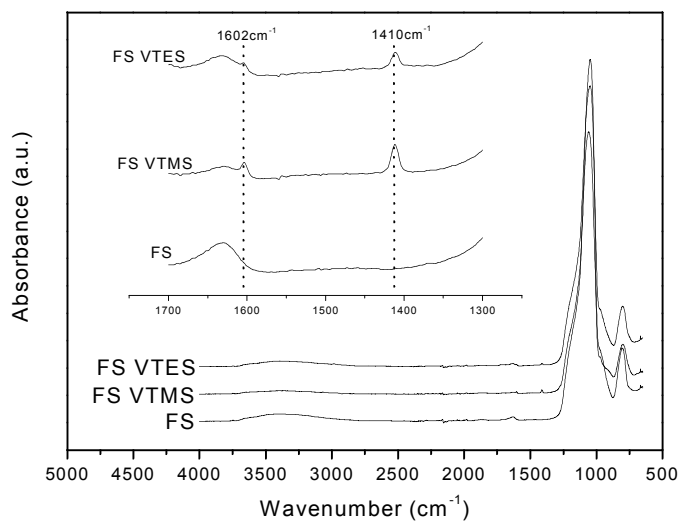


Fig.2

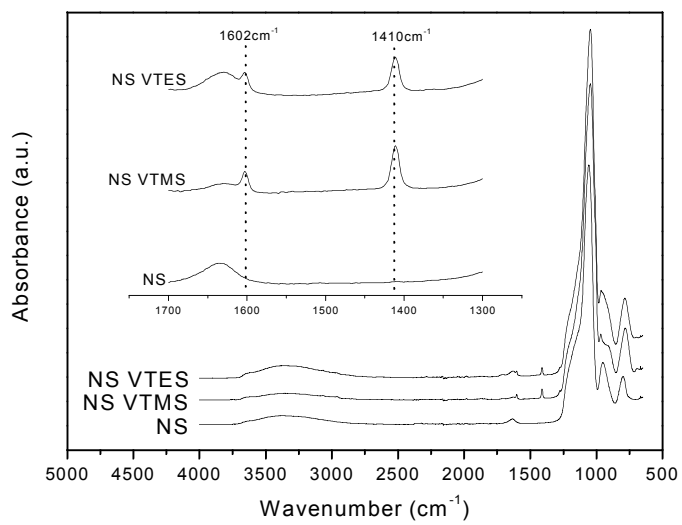


Fig.3

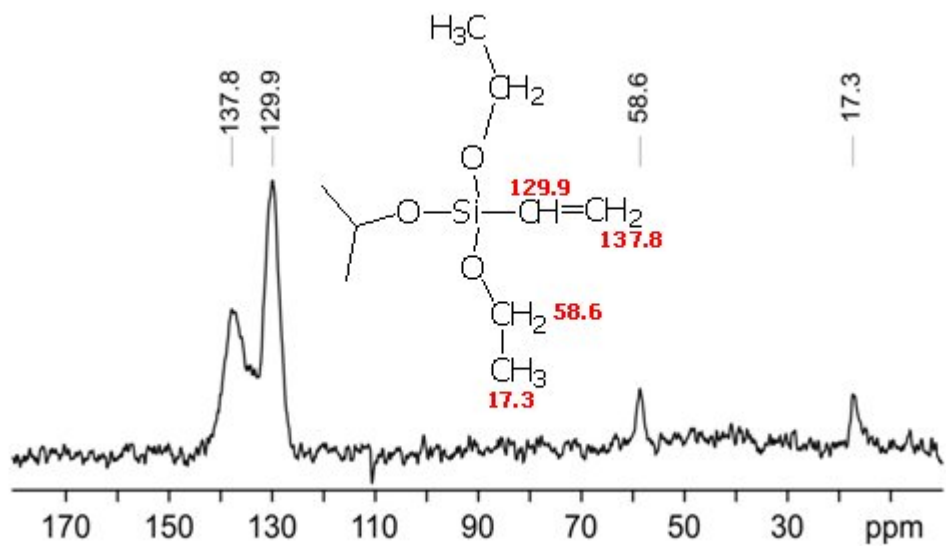
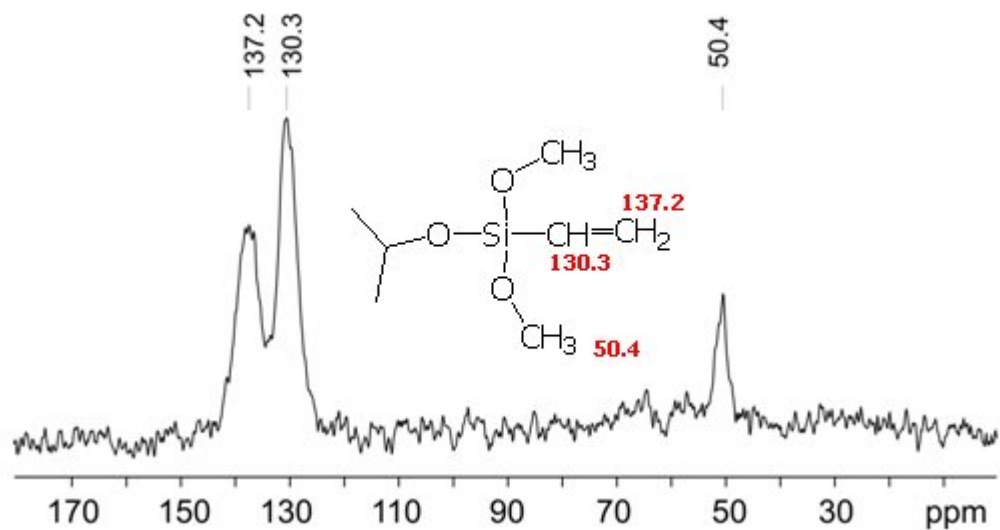


Fig.4

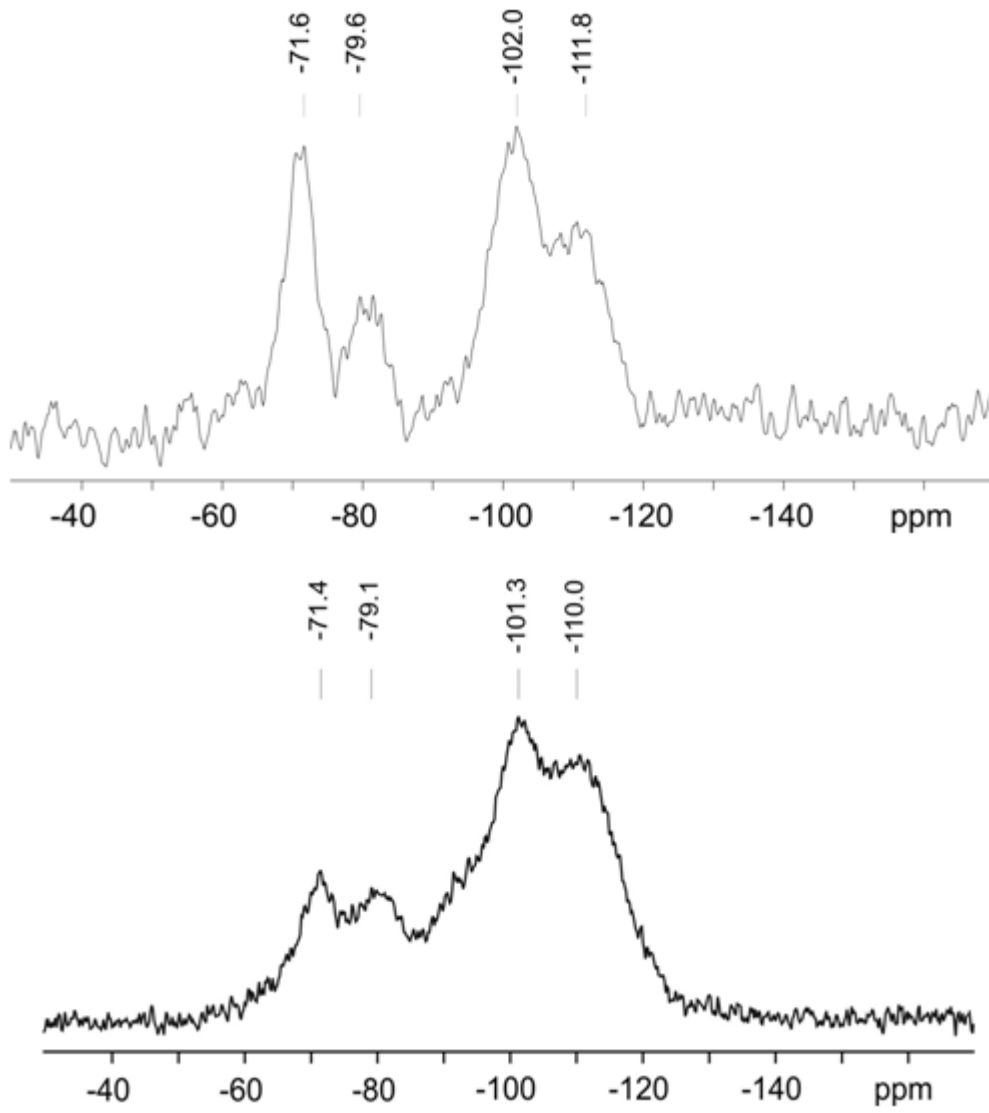


Fig.5

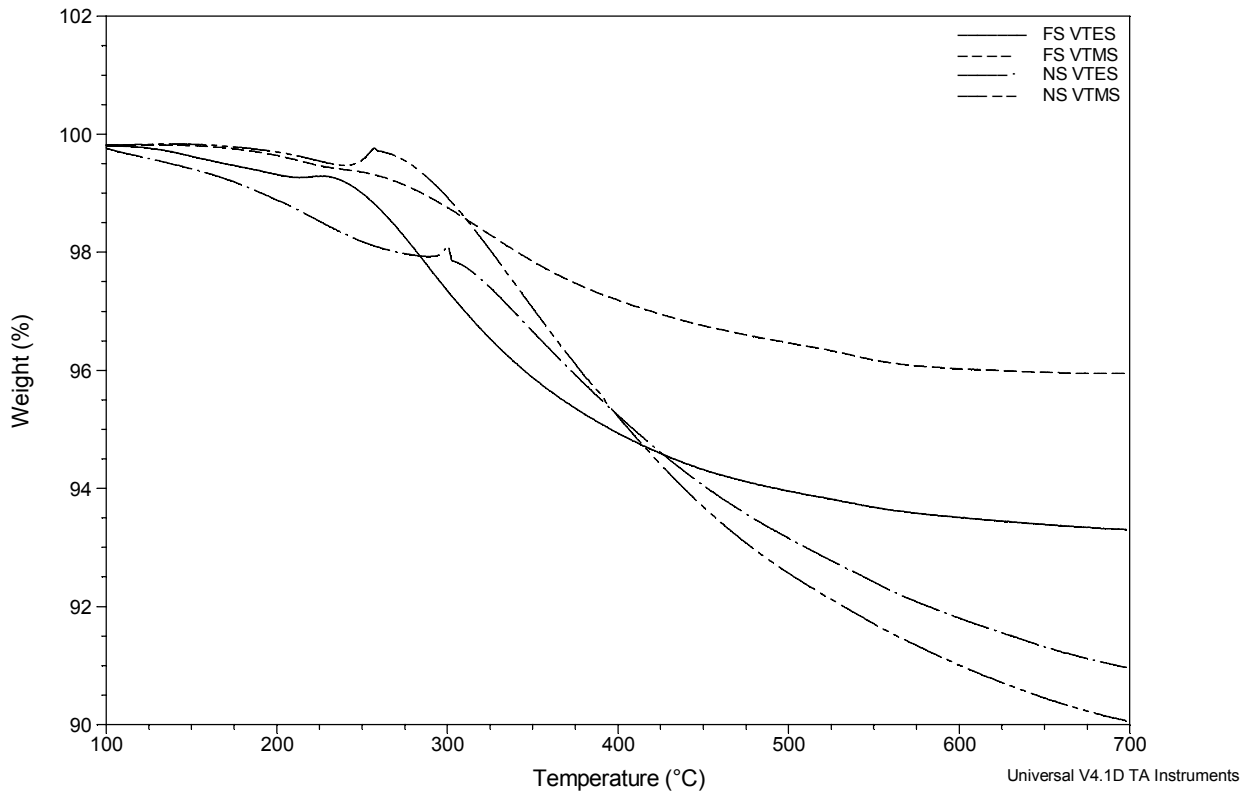


Fig.6

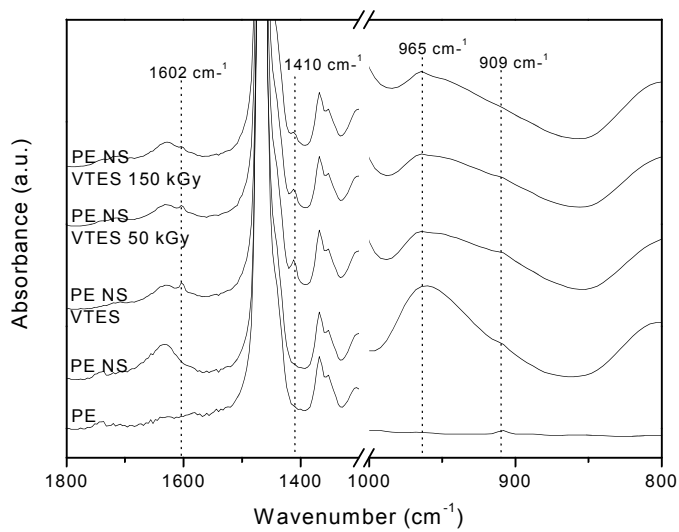


Fig.7

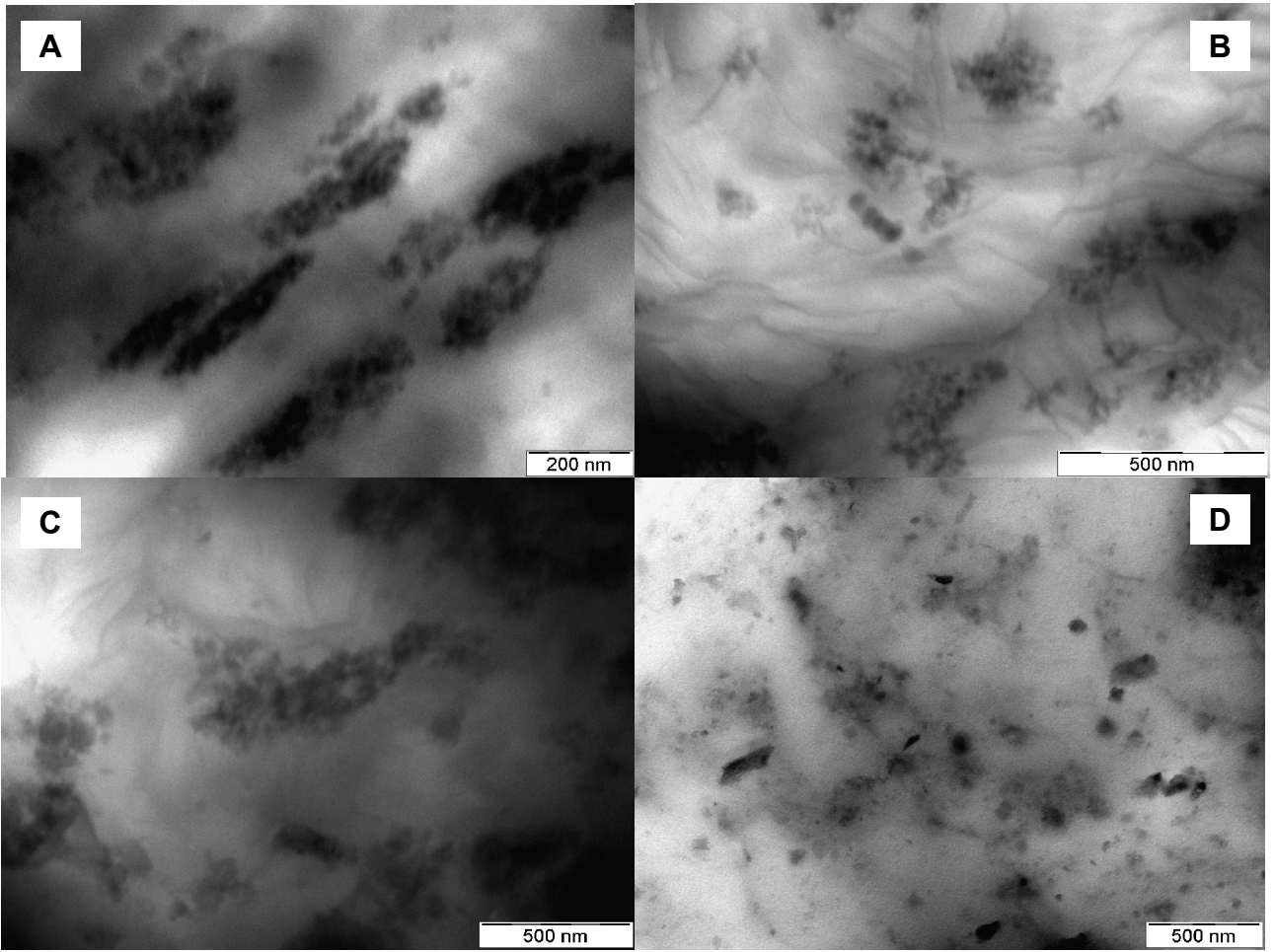


Fig.8

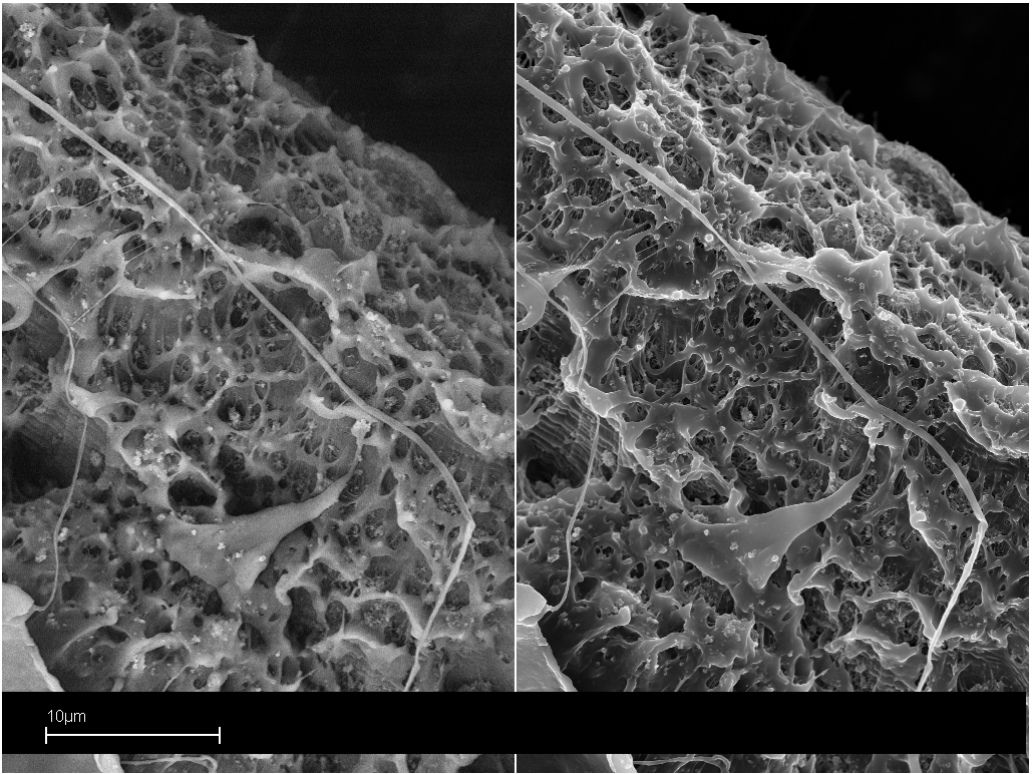


Fig.9

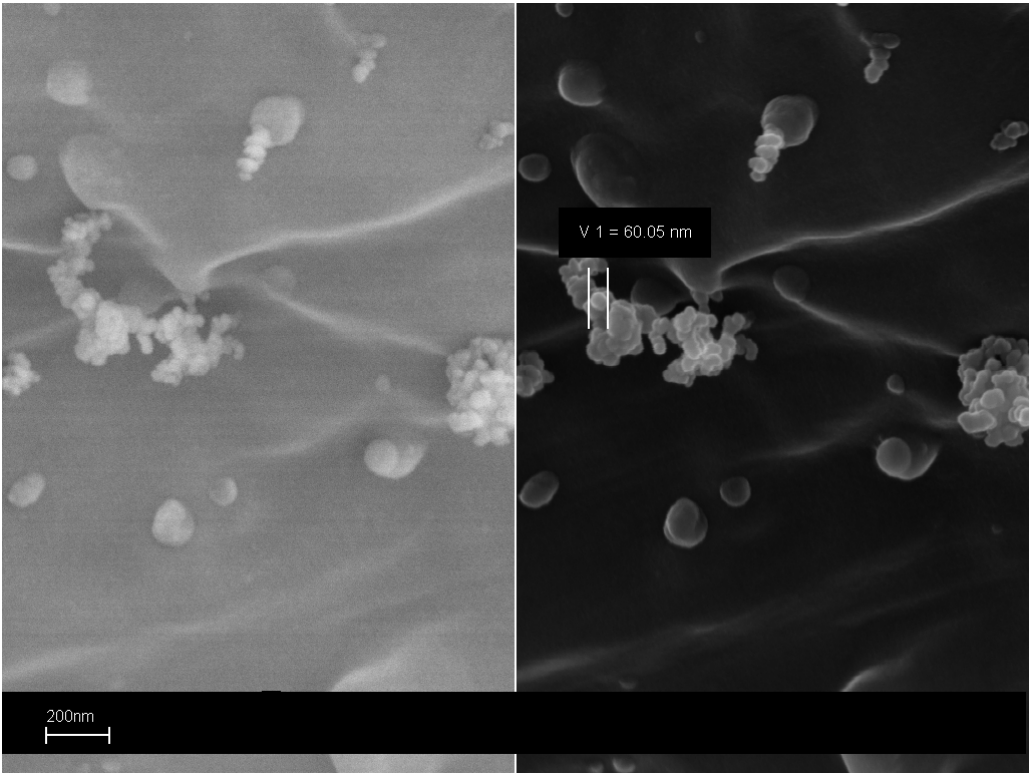


Fig.10

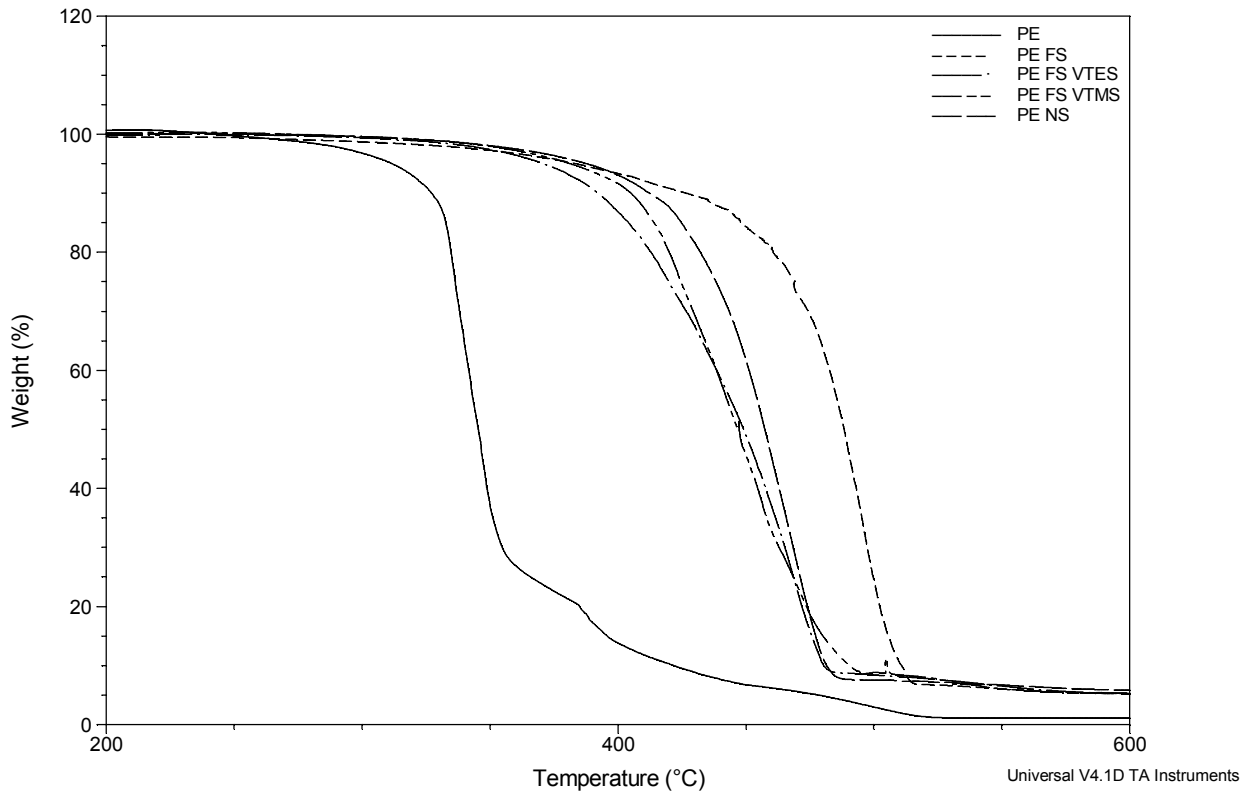


Fig.11

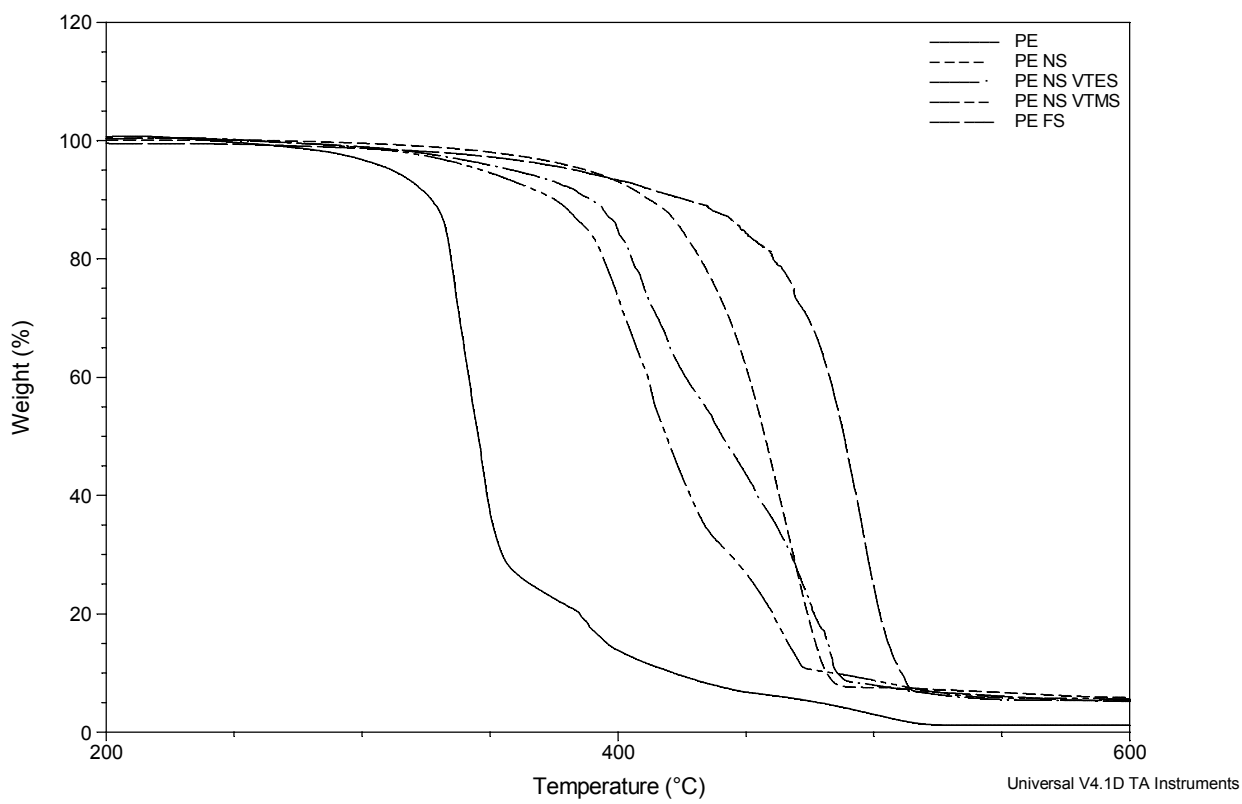


Fig.12

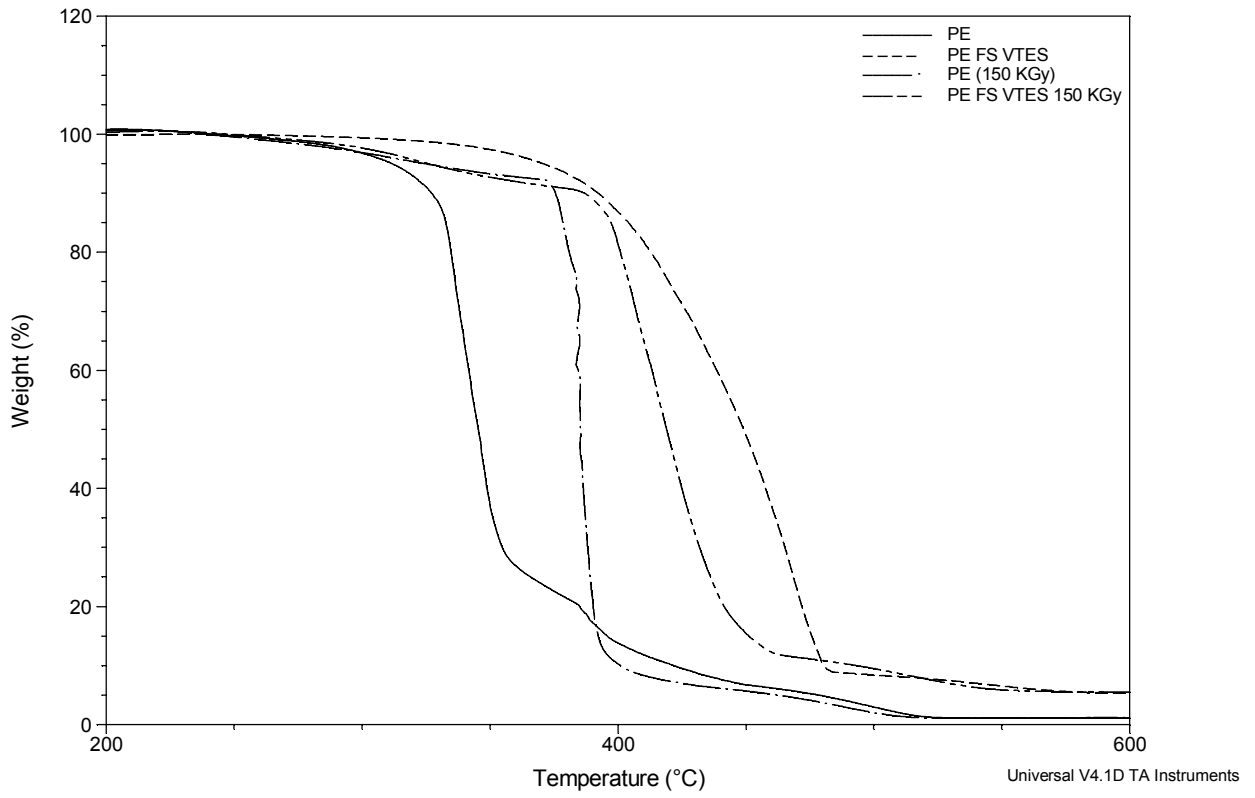


Fig.13

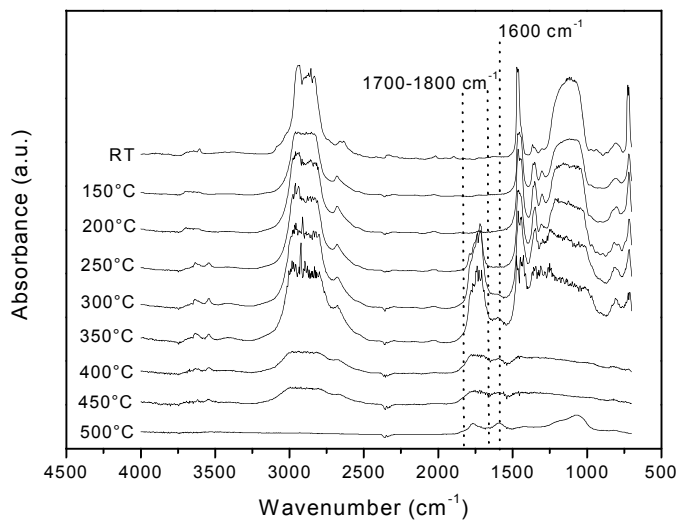
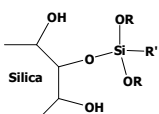
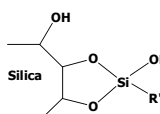
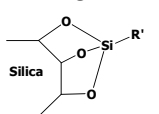
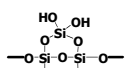
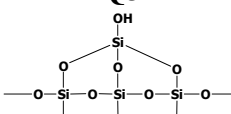
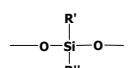
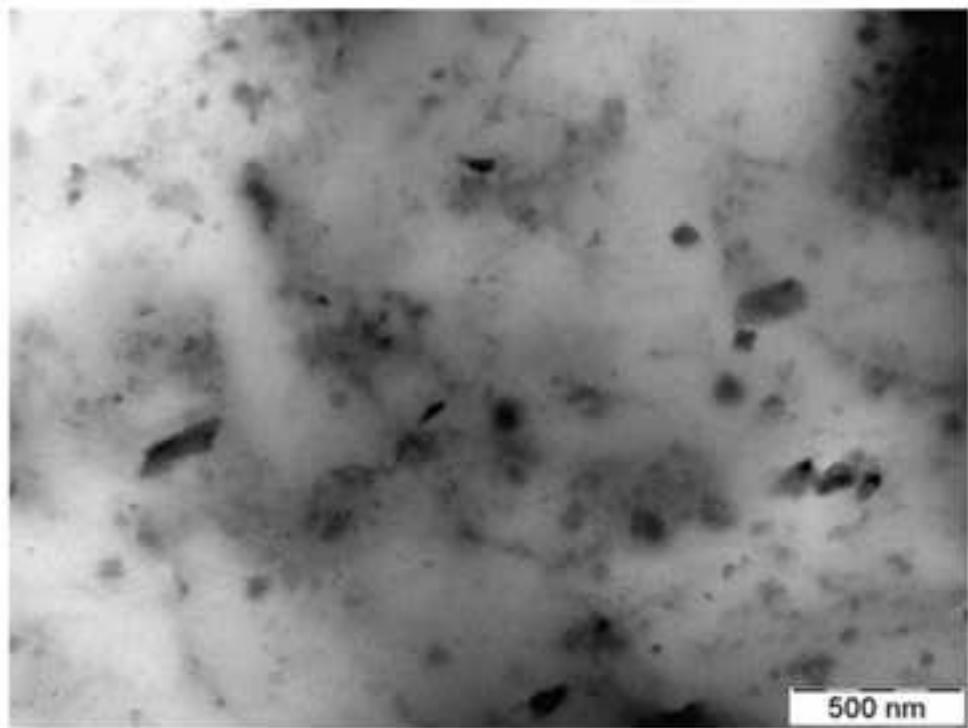
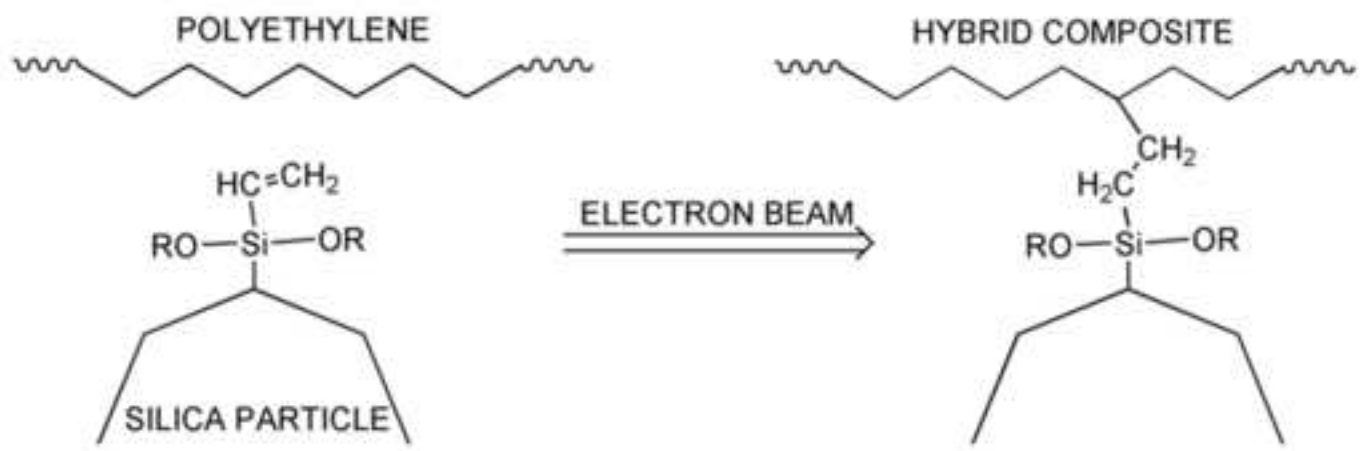


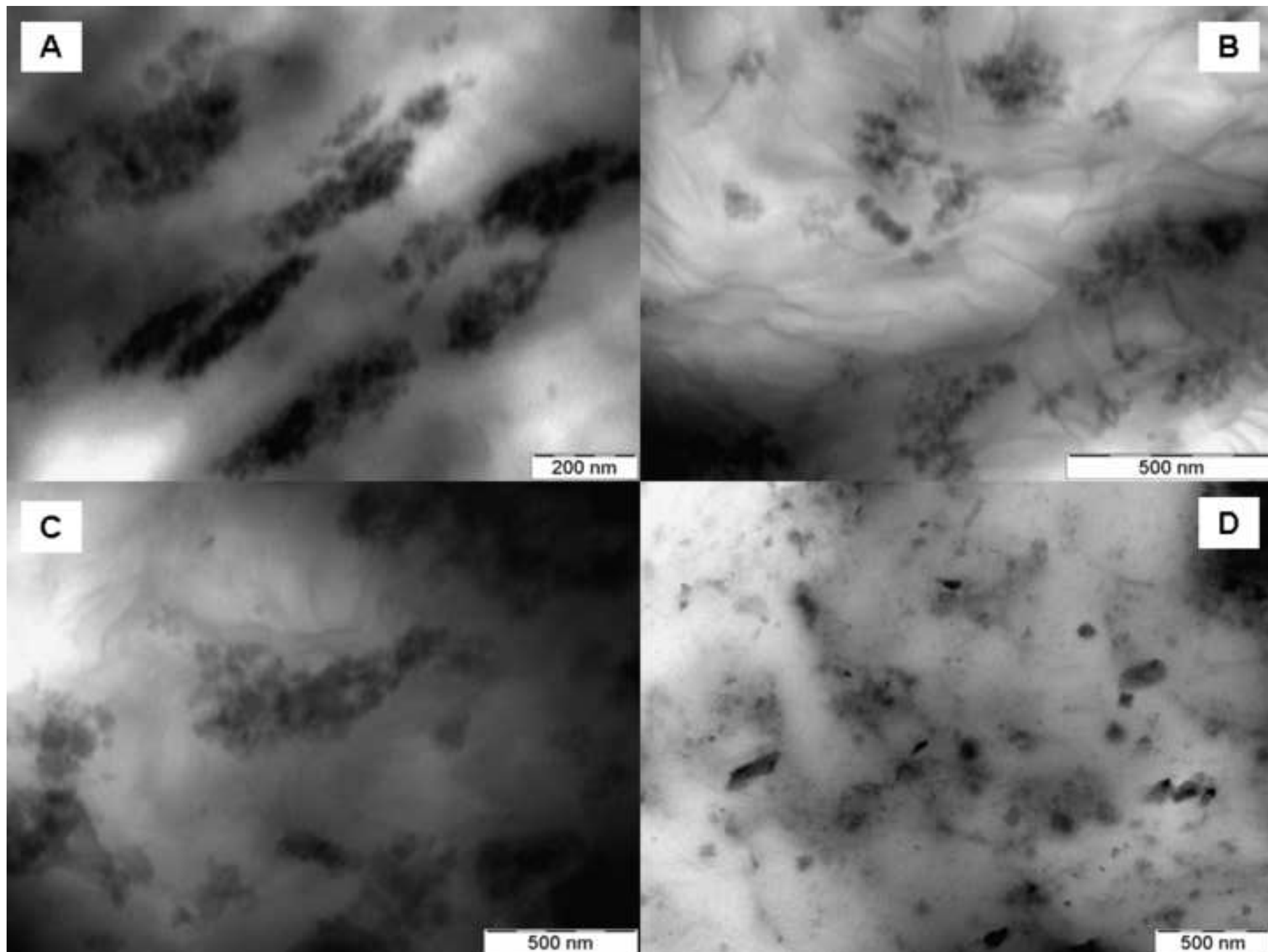
Fig.14

	T1	T2	T3	Q2	Q3	Q4
						
SiO₂				-90.2	-100.2	-108.9
SiO₂-VTMS		-71.6	-79.6		-102.0	-111.8
SiO₂-VTES		-71.4	-79.1		-101.3	-110.0

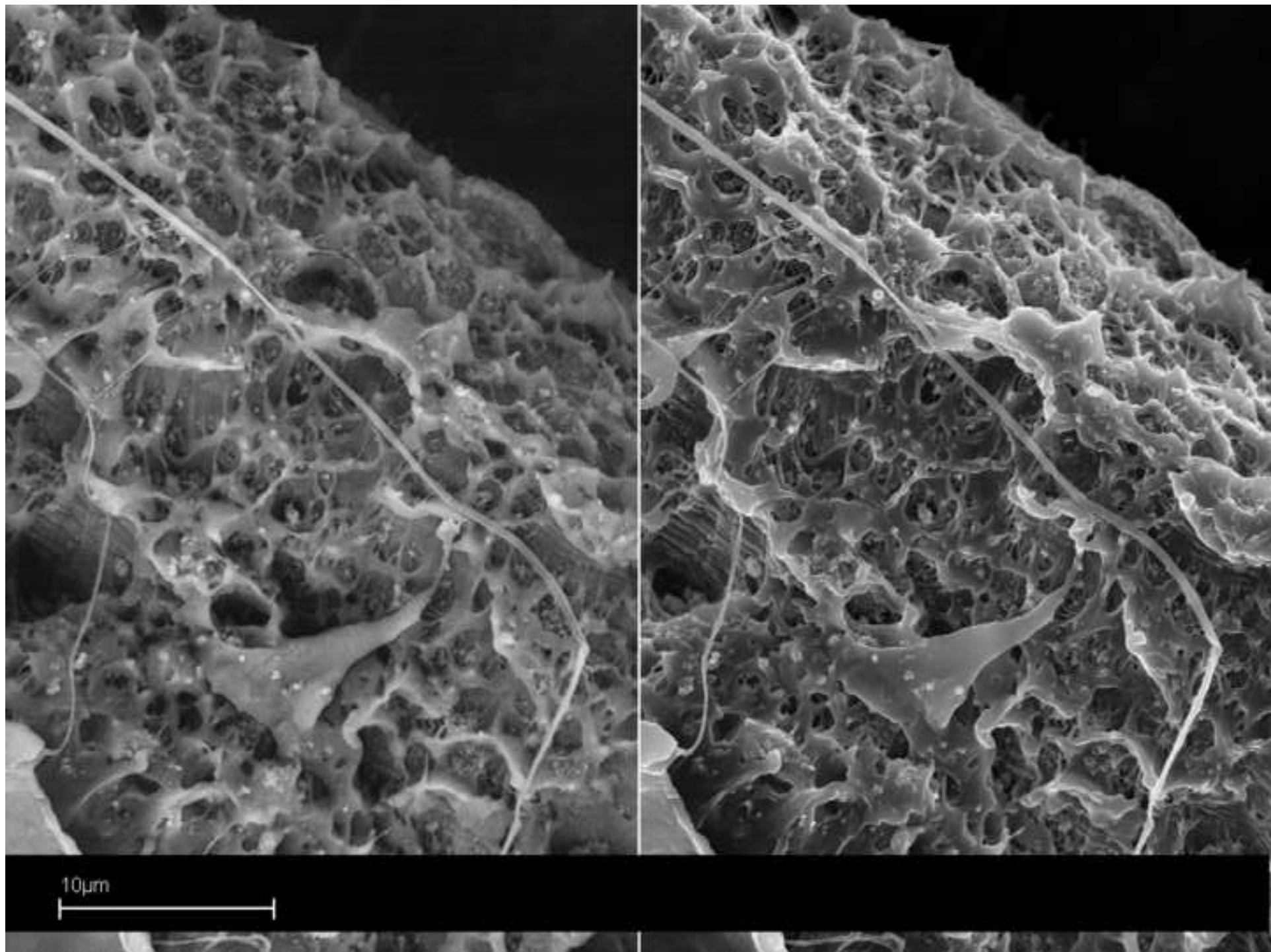
Tab.1



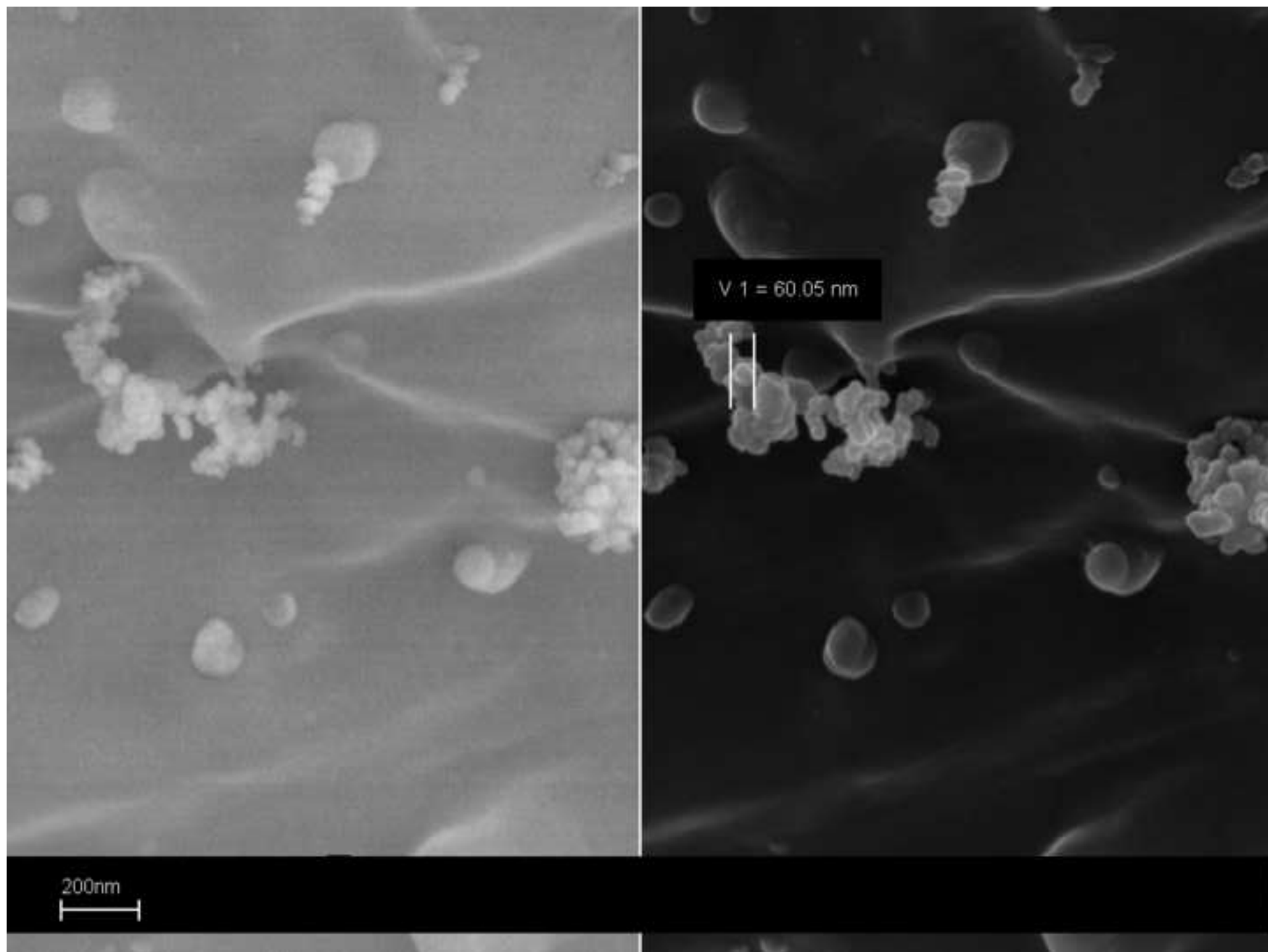
Figure(s)
[Click here to download high resolution image](#)

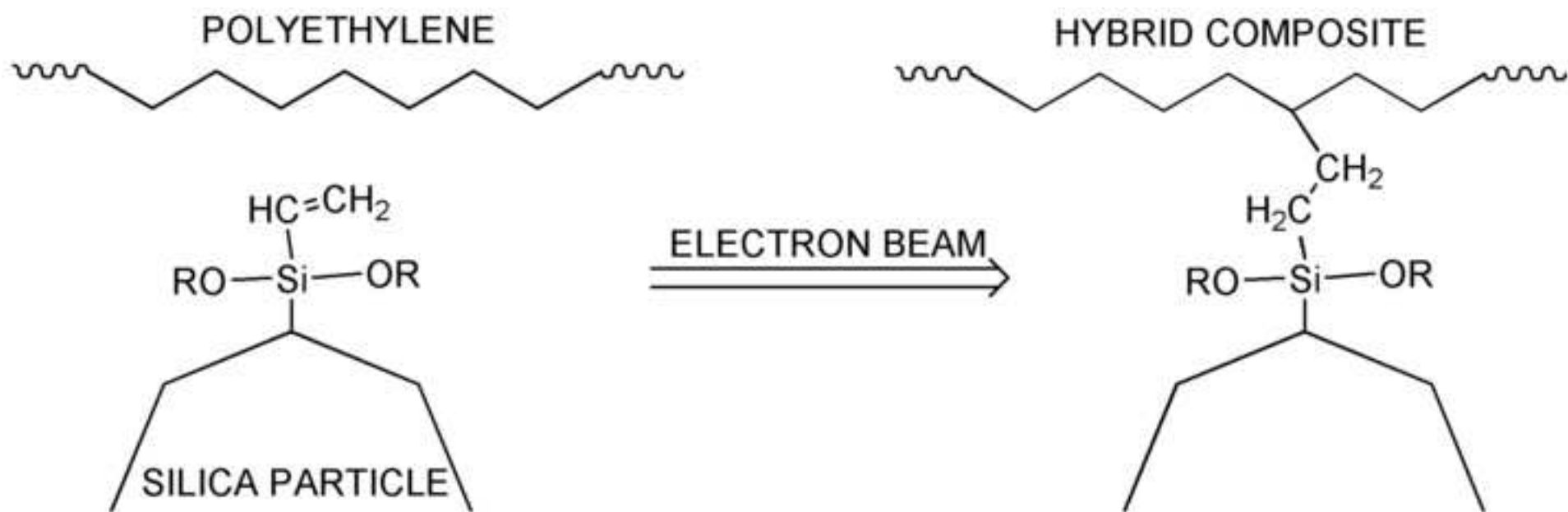


Figure(s)
[Click here to download high resolution image](#)



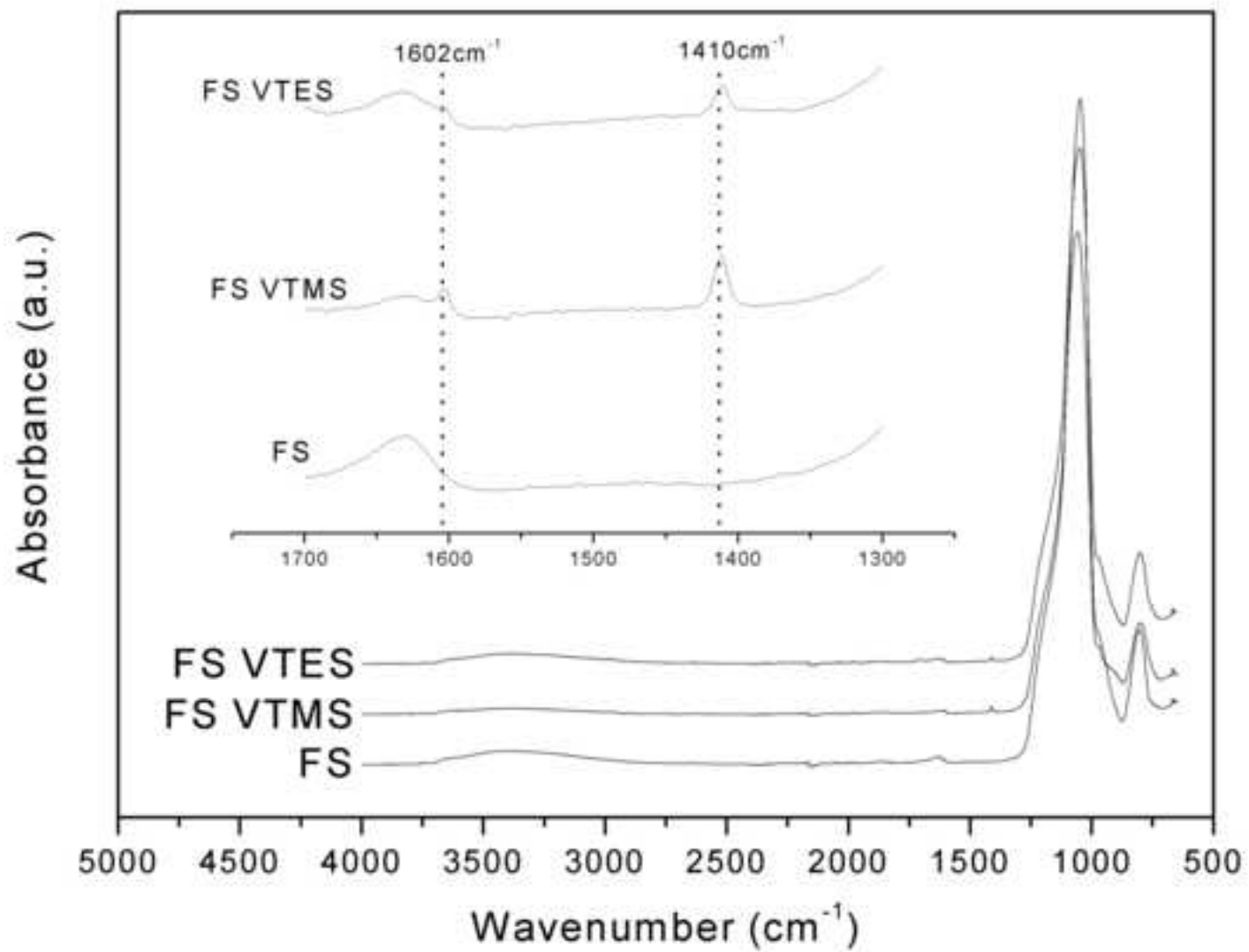
Figure(s)
[Click here to download high resolution image](#)



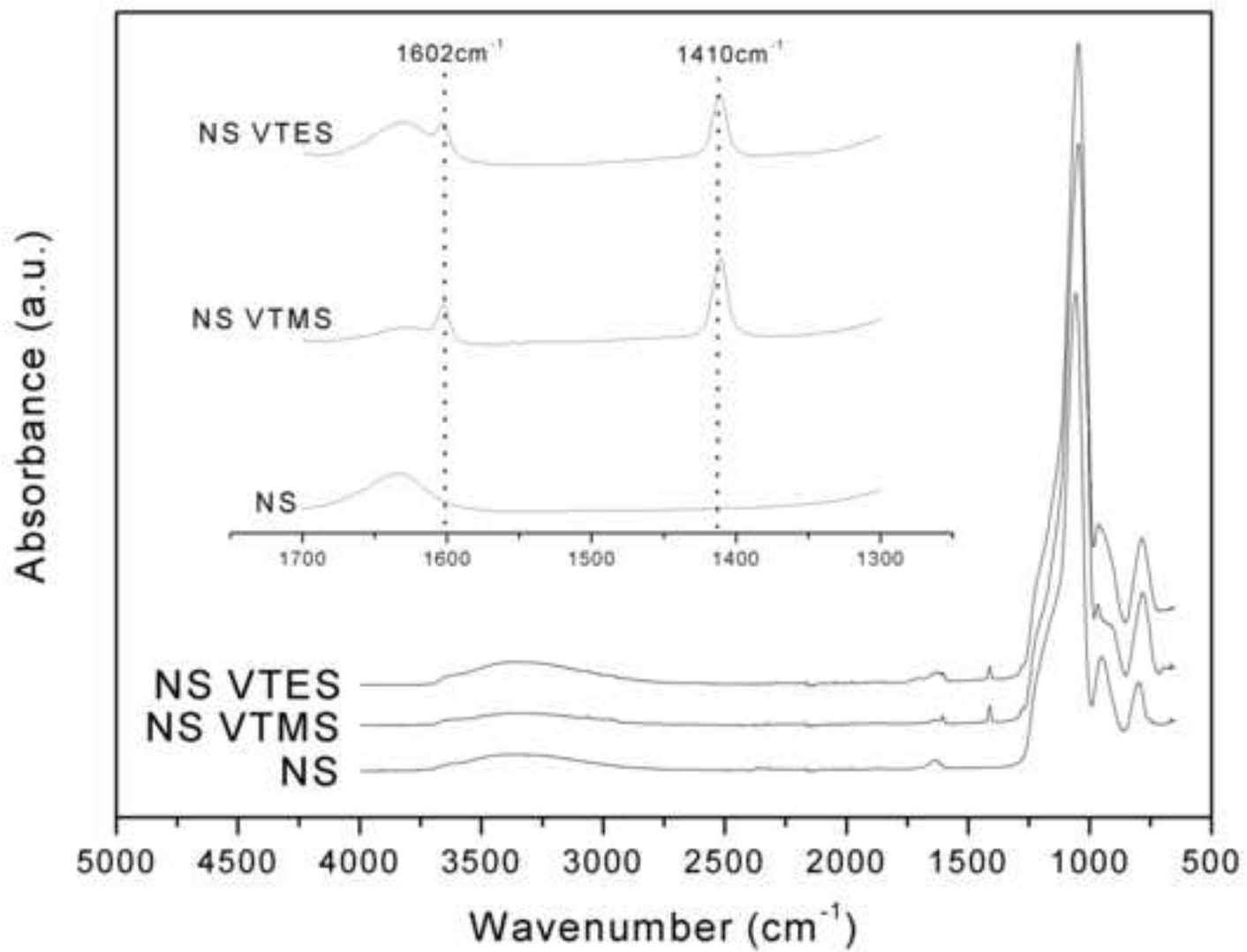


Figure(s)

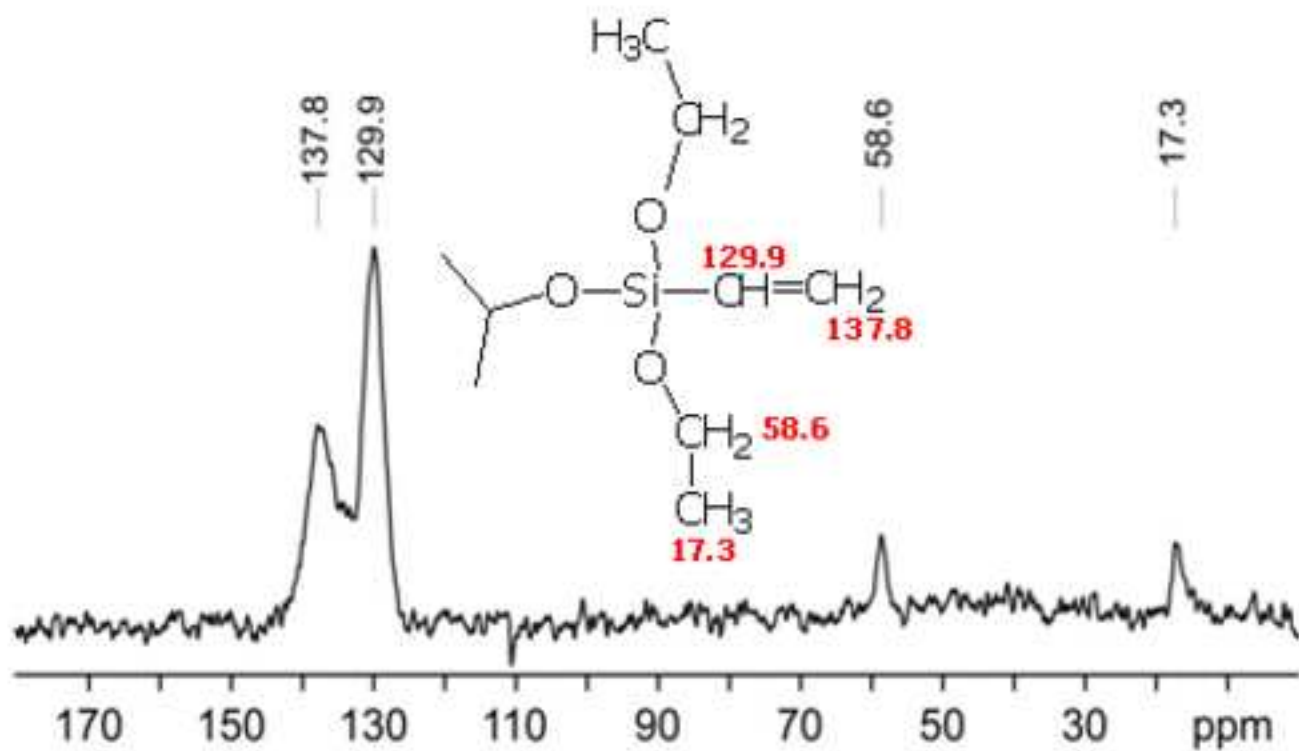
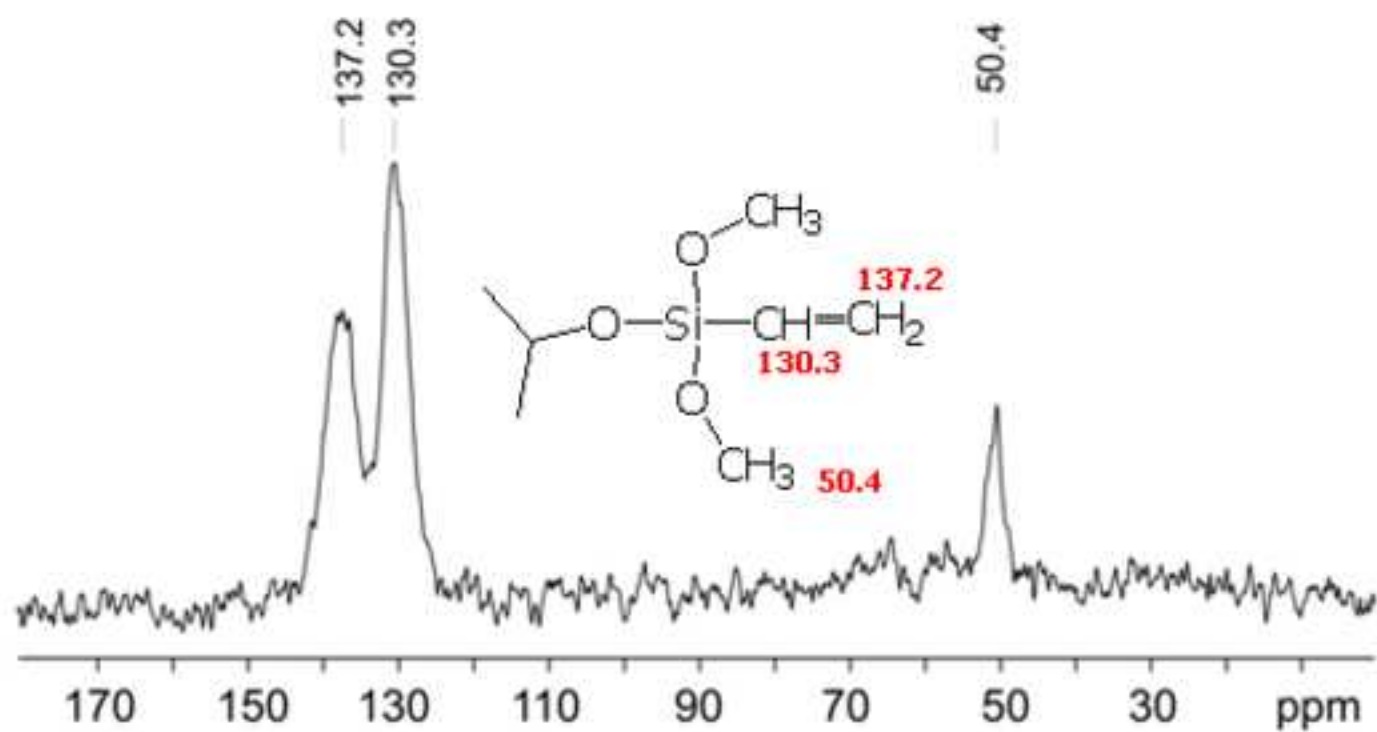
[Click here to download high resolution image](#)



Figure(s)
[Click here to download high resolution image](#)

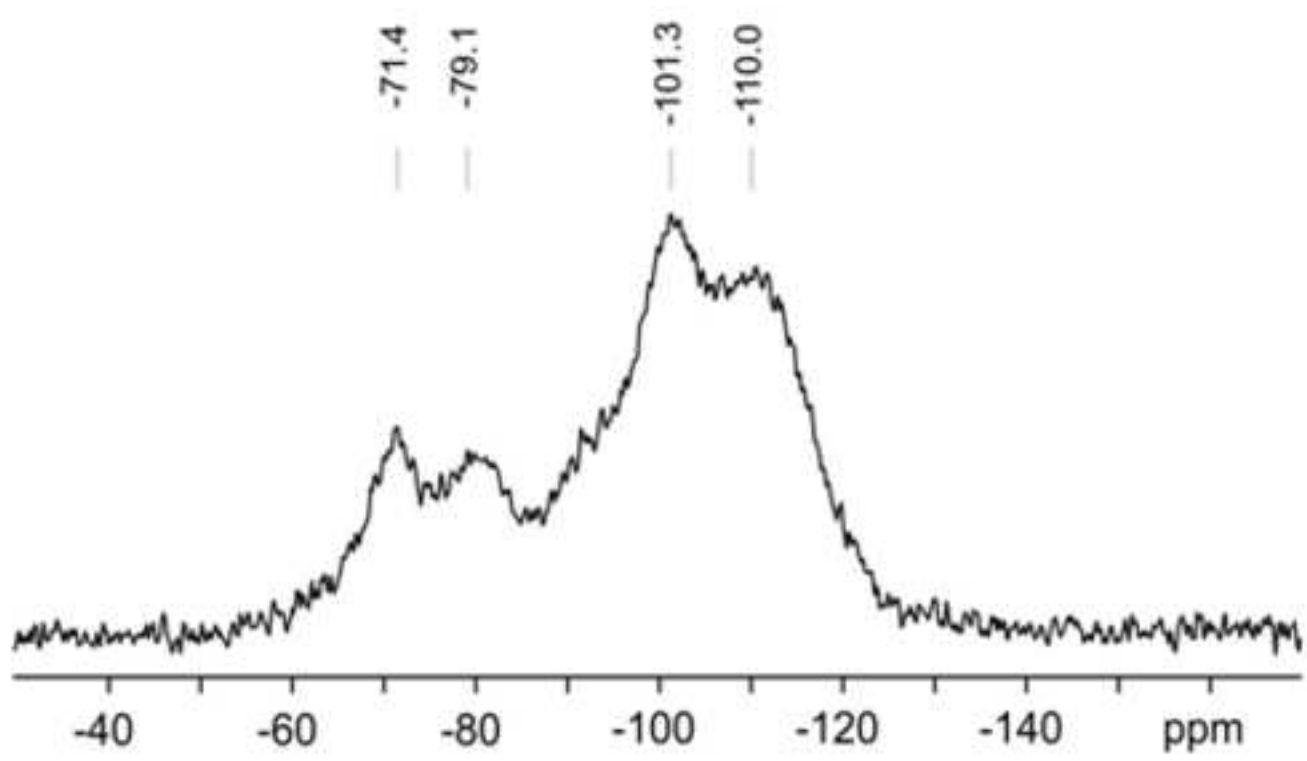
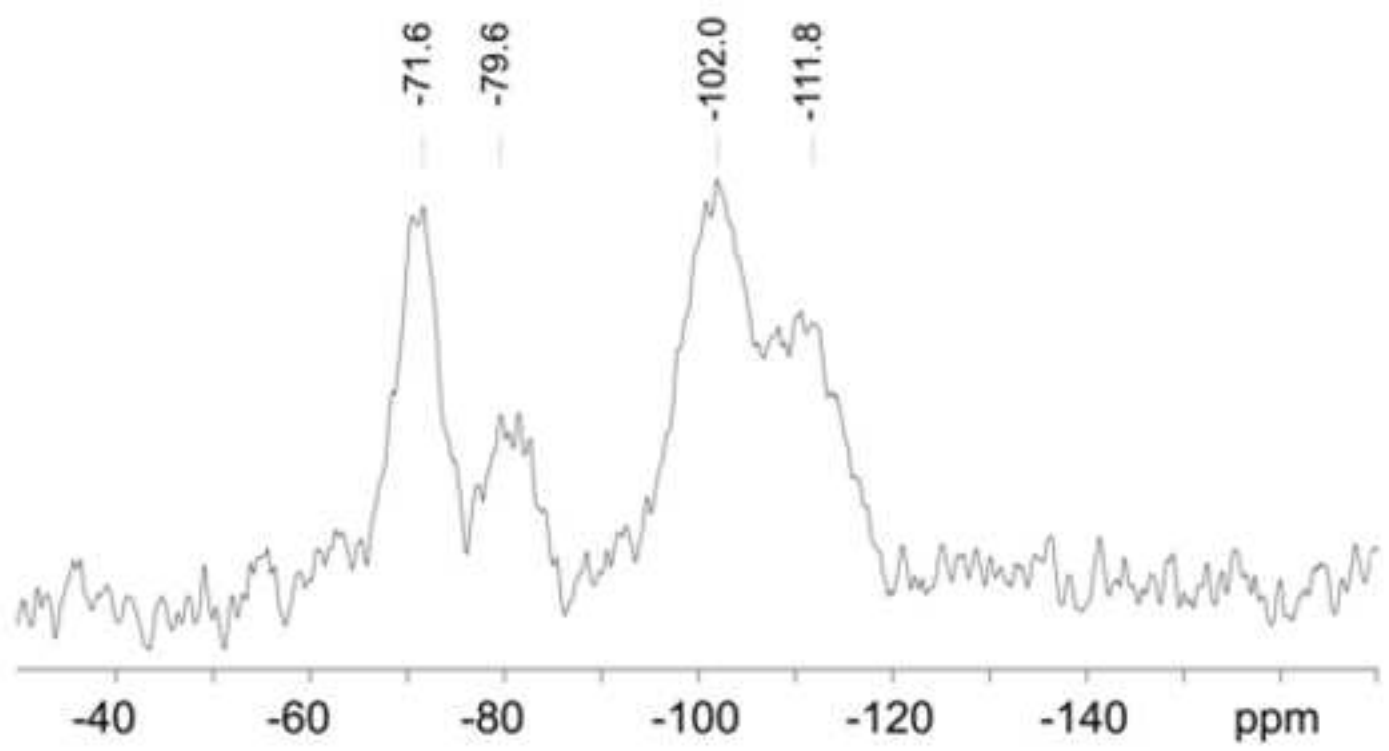


Figure(s)

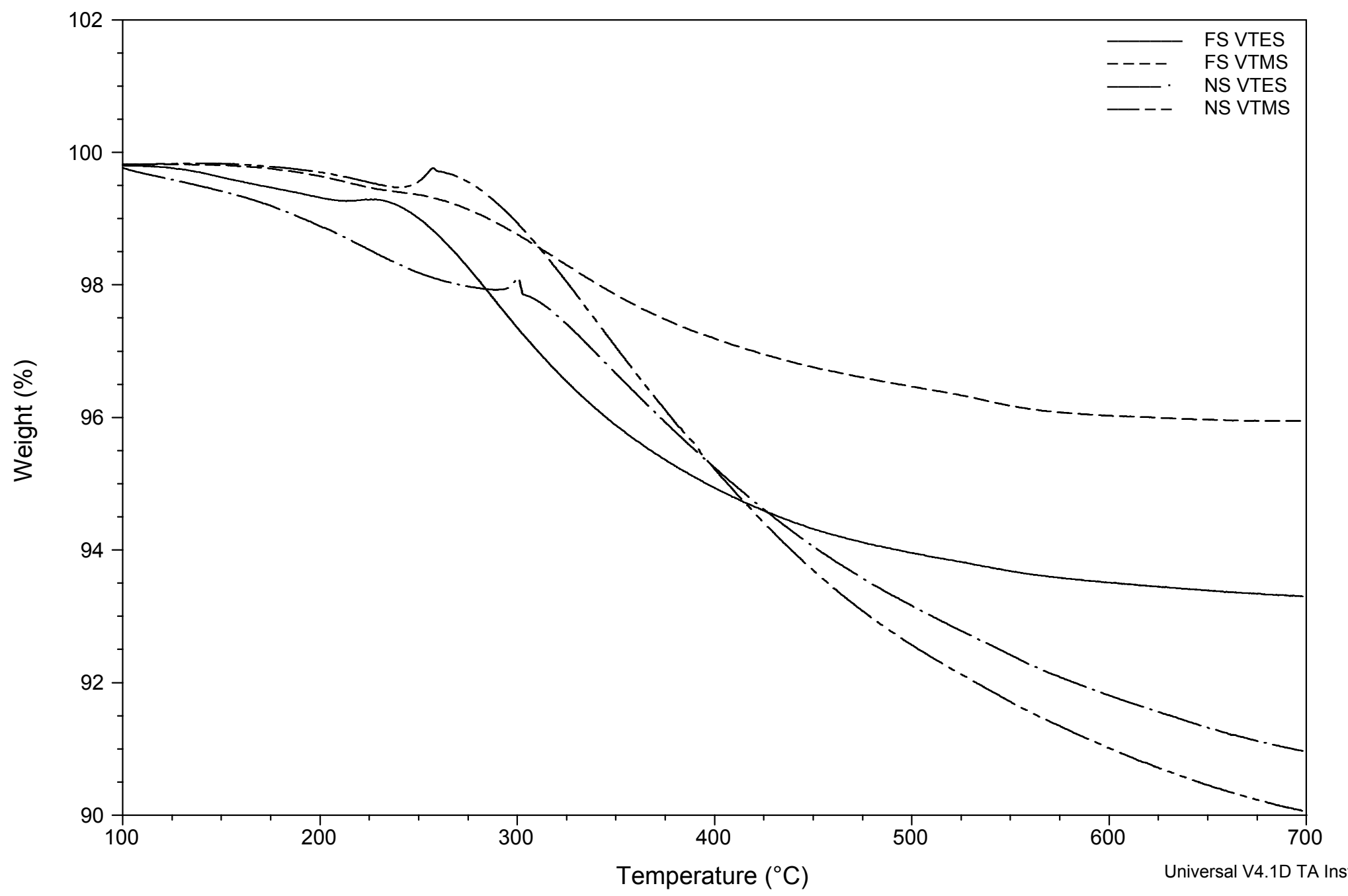
[Click here to download high resolution image](#)

Figure(s)

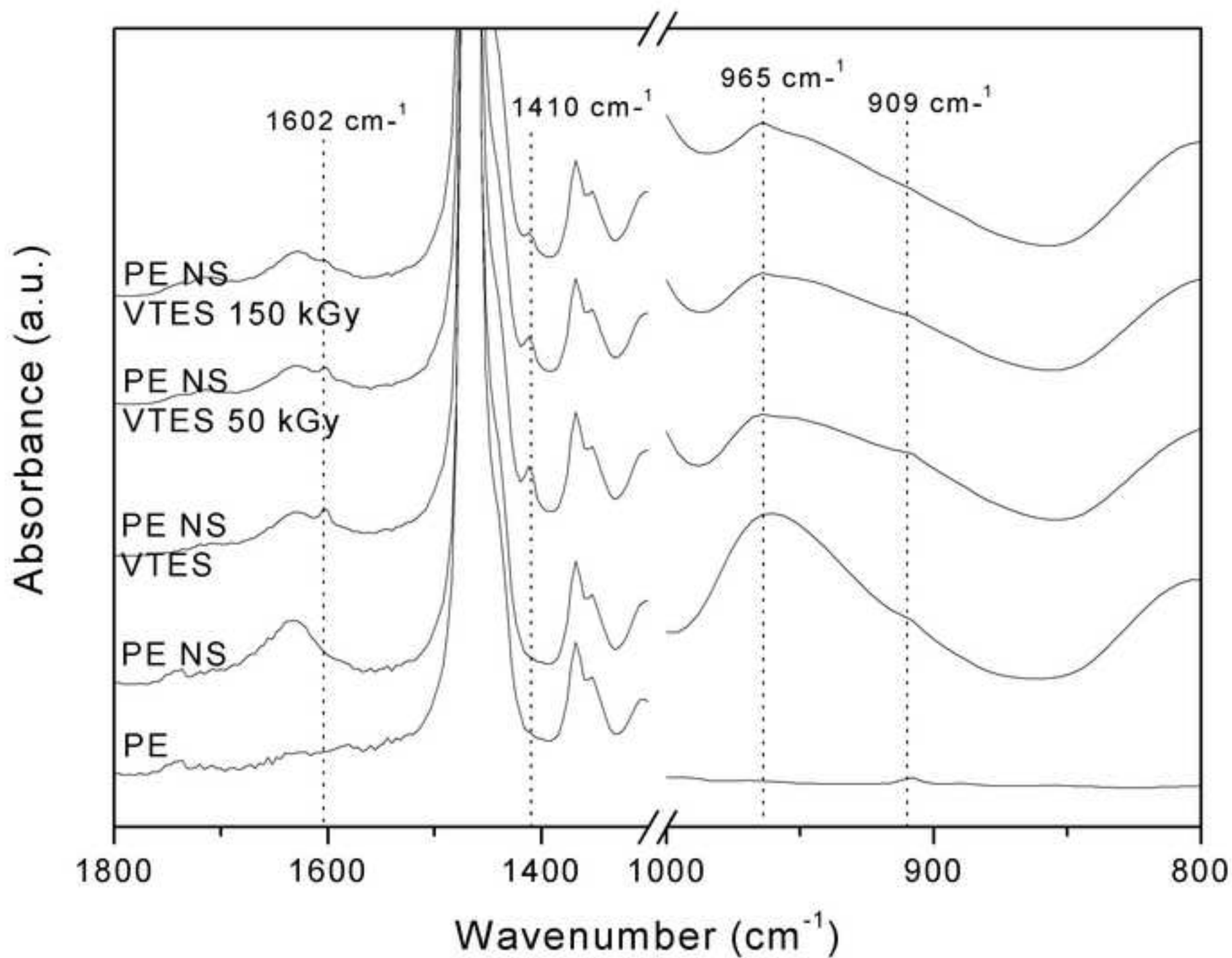
[Click here to download high resolution image](#)



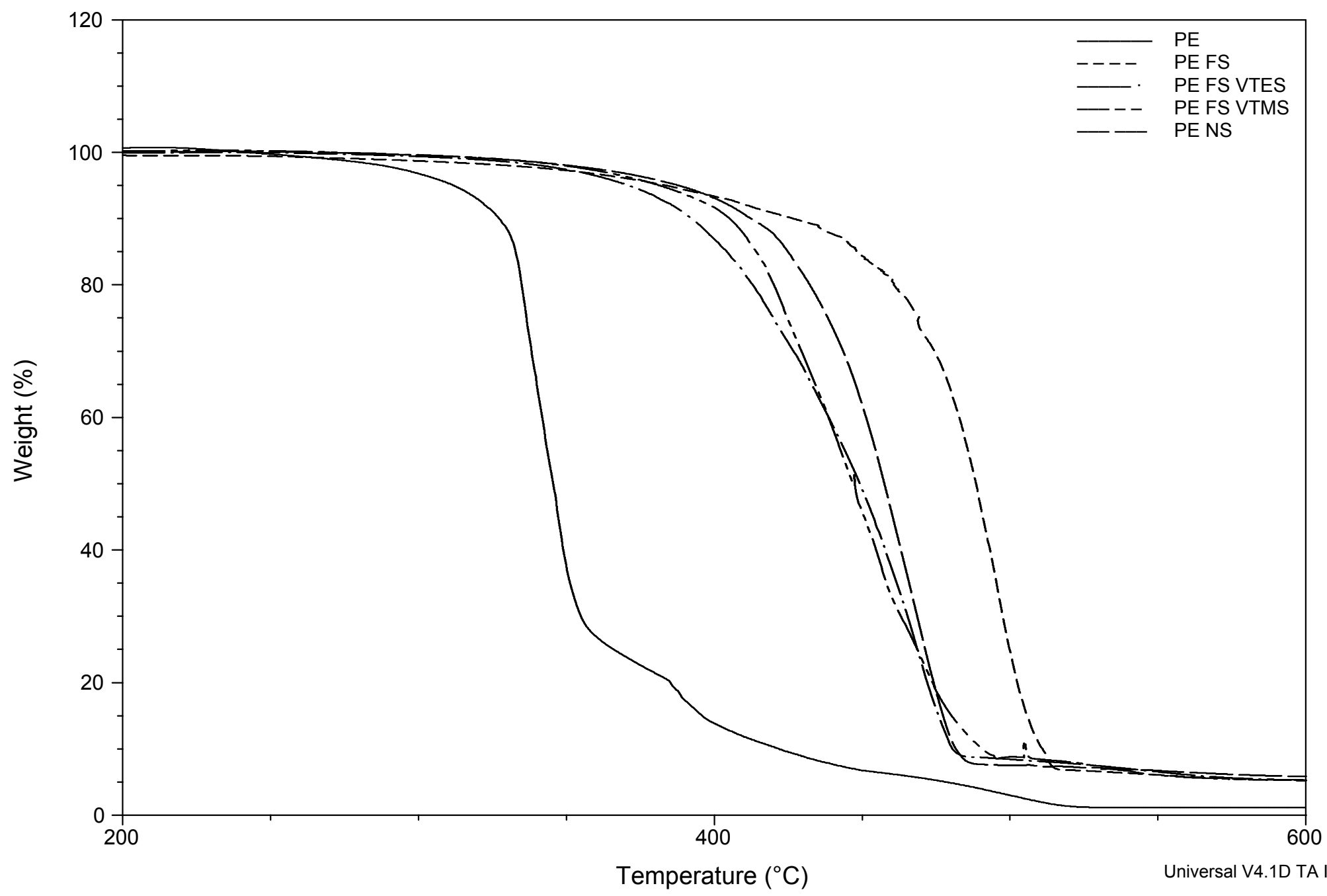
Figure(s)



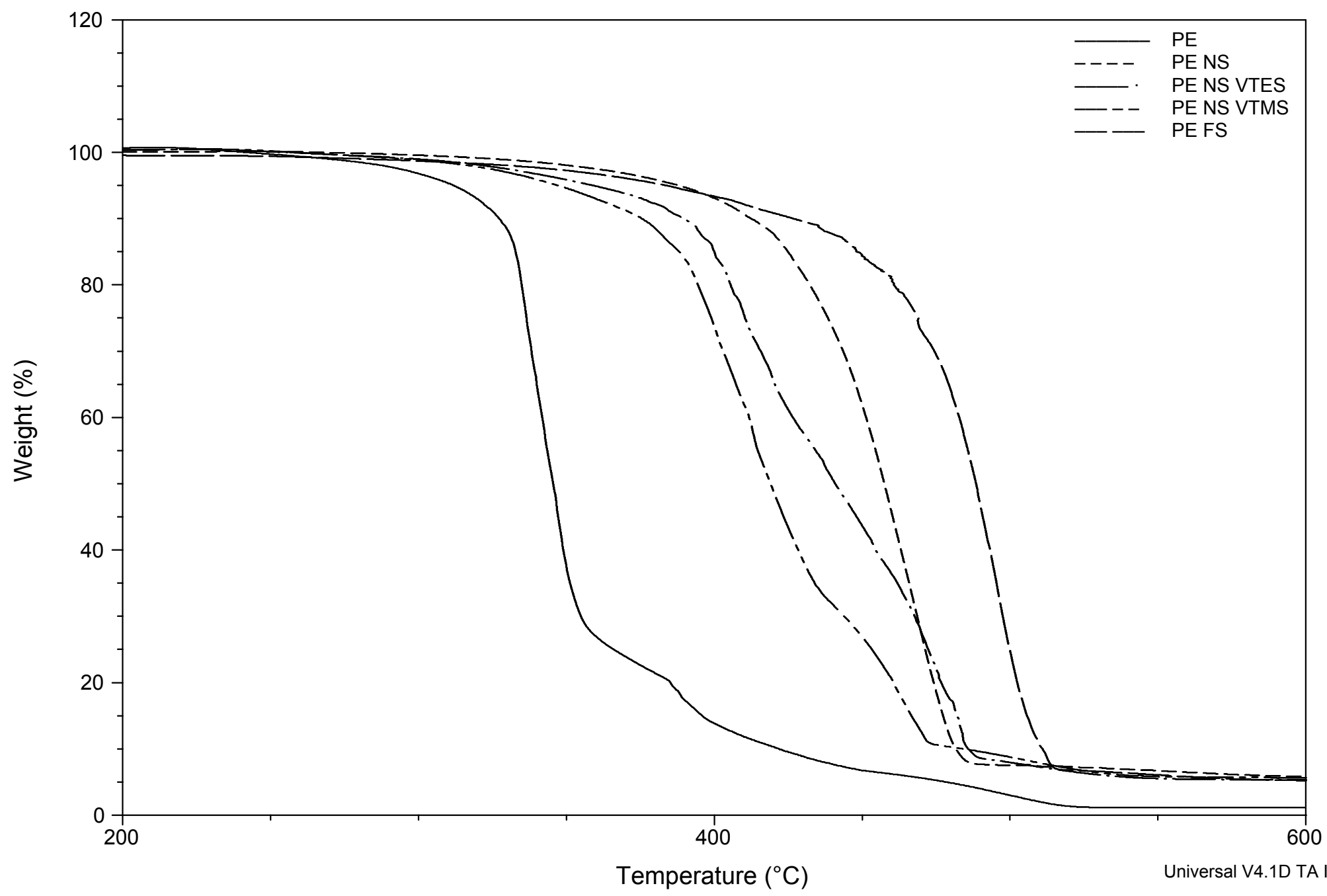
Figure(s)
[Click here to download high resolution image](#)



Figure(s)



Figure(s)



Figure(s)

